doi:10.1093/brain/awaa148 BRAIN 2020: 143; 2235–2254 | 2235

BRAIN
A JOURNAL OF NEUROLOGY

The structural connectivity of subthalamic deep brain stimulation correlates with impulsivity in Parkinson's disease

Philip E. Mosley,[1,2,3,4] Saee Paliwal,[5] Katherine Robinson,[1] Terry Coyne,[3,6] Peter Silburn,[2,3] Marc Tittgemeyer,[7] Klaas E. Stephan,[5,7,8] Alistair Perry,[1,9,10,*] and Michael Breakspear[1,11,*]

*These authors contributed equally to this work.

See Dagher (doi:10.1093/brain/awaa187) for a scientific commentary on this article.

Subthalamic deep brain stimulation (STN-DBS) for Parkinson's disease treats motor symptoms and improves quality of life, but can be complicated by adverse neuropsychiatric side-effects, including impulsivity. Several clinically important questions remain unclear: can 'at-risk' patients be identified prior to DBS; do neuropsychiatric symptoms relate to the distribution of the stimulation field; and which brain networks are responsible for the evolution of these symptoms? Using a comprehensive neuropsychiatric battery and a virtual casino to assess impulsive behaviour in a naturalistic fashion, 55 patients with Parkinson's disease (19 females, mean age 62, mean Hoehn and Yahr stage 2.6) were assessed prior to STN-DBS and 3 months postoperatively. Reward evaluation and response inhibition networks were reconstructed with probabilistic tractography using the participant-specific subthalamic volume of activated tissue as a seed. We found that greater connectivity of the stimulation site with these frontostriatal networks was related to greater postoperative impulsiveness and disinhibition as assessed by the neuropsychiatric instruments. Larger bet sizes in the virtual casino postoperatively were associated with greater connectivity of the stimulation site with right and left orbitofrontal cortex, right ventromedial prefrontal cortex and left ventral striatum. For all assessments, the baseline connectivity of reward evaluation and response inhibition networks prior to STN-DBS was not associated with postoperative impulsivity; rather, these relationships were only observed when the stimulation field was incorporated. This suggests that the site and distribution of stimulation is a more important determinant of postoperative neuropsychiatric outcomes than preoperative brain structure and that stimulation acts to mediate impulsivity through differential recruitment of frontostriatal networks. Notably, a distinction could be made amongst participants with clinically-significant, harmful changes in mood and behaviour attributable to DBS, based upon an analysis of connectivity and its relationship with gambling behaviour. Additional analyses suggested that this distinction may be mediated by the differential involvement of fibres connecting ventromedial subthalamic nucleus and orbitofrontal cortex. These findings identify a mechanistic substrate of neuropsychiatric impairment after STN-DBS and suggest that tractography could be used to predict the incidence of adverse neuropsychiatric effects. Clinically, these results highlight the importance of accurate electrode placement and careful stimulation titration in the prevention of neuropsychiatric side-effects after STN-DBS.

1 Systems Neuroscience Group, QIMR Berghofer Medical Research Institute, Herston, Queensland, Australia
2 Neurosciences Queensland, St Andrew's War Memorial Hospital, Spring Hill, Queensland, Australia
3 Queensland Brain Institute, University of Queensland, St Lucia, Queensland, Australia
4 Faculty of Medicine, University of Queensland, Herston, Queensland, Australia
5 Translational Neuromodeling Unit (TNU), Institute for Biomedical Engineering, University of Zürich and Swiss Federal Institute of Technology (ETH Zürich), Zürich, Switzerland
6 Brizbrain and Spine, The Wesley Hospital, Auchenflower, Queensland, Australia

Received November 18, 2019. Revised March 19, 2020. Accepted March 20, 2020. Advance access publication June 22, 2020

7 Max Planck Institute for Metabolism Research, Cologne, Germany
8 Wellcome Centre for Human Neuroimaging, University College London, London, UK
9 Max Planck UCL Centre for Computational Psychiatry and Ageing Research, Berlin, Germany
10 Centre for Lifespan Psychology, Max Planck Institute for Human Development, Berlin, Germany
11 Brain and Mind Priority Research Centre, Hunter Medical Research Institute, University of Newcastle, NSW, Australia

Correspondence to: Dr Philip E. Mosley
Neurosciences Queensland, Level 1, St Andrew's Place, 33 North Street, Spring Hill
Queensland, 4000, Australia
E-mail: philip.mosley@qimrberghofer.edu.au

Keywords: deep brain stimulation; subthalamic nucleus; impulsivity; Parkinson's disease; gambling

Abbreviations: DBS = deep brain stimulation; ICB = impulse control behaviour; IFG = inferior frontal gyrus; OFC = orbitofrontal cortex; SMA = supplementary motor area; STN = subthalamic nucleus; VAT = volume of activated tissue; vmPFC = ventromedial prefrontal cortex; VTA = ventral tegmental area

Introduction

Deep brain stimulation (DBS) of the subthalamic nucleus (STN) in Parkinson's disease is an established advanced therapy that treats motor symptoms (tremor, rigidity, bradykinesia), improves quality of life, and permits reduction or cessation of dopaminergic therapies (Krack *et al.*, 2003; Williams *et al.*, 2010; Schuepbach *et al.*, 2013). However, in a proportion of those treated with STN-DBS, stimulation may induce neuropsychiatric symptoms, most often characterized by impulsivity and mood elevation (Romito *et al.*, 2002; Daniele *et al.*, 2003; Hershey *et al.*, 2004, 2010; Voon *et al.*, 2006; Appleby *et al.*, 2007; Mallet *et al.*, 2007; Welter *et al.*, 2014; Mosley and Marsh, 2015). Although these symptoms can be ameliorated with stimulation reprogramming, they may nonetheless be associated with lasting harm (Mosley *et al.*, 2018*b*, 2019*b*) and caregiver burden (Mosley *et al.*, 2018*a*).

The ability to predict those at risk of a poor non-motor outcome would be a significant benefit to clinicians delivering this therapy, affecting surgical candidacy and choice of target. This is because the internal segment of the globus pallidus represents an alternative DBS site that has been advanced as a neuropsychiatrically 'safer' target (Okun and Foote, 2005) but with potentially less favourable motor outcomes (Odekerken *et al.*, 2013). Unfortunately, most preoperative measures show poor sensitivity and specificity for this syndrome. Whilst impulse control behaviours (ICBs) related to dopaminergic therapy display the greatest phenomenological overlap with stimulation-induced neuropsychiatric symptoms, their presence is not predictive and their absence is not protective: patients with pre-DBS ICBs may remit after STN-DBS following medication reduction (Lhommee *et al.*, 2012; Eusebio *et al.*, 2013), whilst those on medication but with no history of ICBs may develop such behaviours after STN-DBS (Lim *et al.*, 2009; Moum *et al.*, 2012).

STN-DBS may facilitate movement in Parkinson's disease by disrupting synchronous oscillations between STN and cortex (Eusebio *et al.*, 2009, 2011; Shimamoto *et al.*, 2013), particularly in the hyperdirect pathway (Nambu *et al.*, 2002; Akram *et al.*, 2017). However, there is evidence to suggest that neuropsychiatric side effects of this therapy may also be determined by modulation of activity in frontostriatal networks. The STN has an internal functional topography, with a motor subregion in the dorsolateral aspect of the nucleus that transitions into cognitive-associative and affective subregions in the ventromedial plane (Lambert *et al.*, 2012; Haynes and Haber, 2013; Accolla *et al.*, 2014; Ewert *et al.*, 2018). Spread of the stimulation field around a DBS electrode in the motor region of the STN can also modulate these non-motor circuits. Previously, by localizing the active DBS contact and modelling a stimulation field based on individualized parameters, we reported an association between stimulation of the cognitive-associative STN subregion and postoperative disinhibition, in addition to the emergence of clinically-significant neuropsychiatric symptoms such as hypomania (Mosley *et al.*, 2018*c*). The physiological underpinnings of this impairment may result from the STN's role as a 'stopping' node in the indirect pathway of the basal ganglia. By inhibiting the output of cortico-striatal circuits, healthy STN firing delays decision-making, allowing time for evidence accumulation and the formulation of an appropriate behavioural policy (Doll and Frank, 2009). Accordingly, overriding this function with DBS may unmask impulsive and error-prone responding (Frank *et al.*, 2007; Cavanagh *et al.*, 2011). More generally, dimensional variations in a range of non-motor symptoms after STN-DBS have been found to covary with the spread of electrical stimulation (Petry-Schmelzer *et al.*, 2019). However, beyond local effects of DBS, a mechanistic association between modulation of frontostriatal networks and the emergence of post-DBS neuropsychiatric symptoms has not been established.

Quantifying the relationship between impulsivity and the individualized connectivity of the subthalamic stimulation field can address this issue. Through modelling the distribution of white matter tracts in the brain, diffusion MRI can be used to investigate connections of the surgical target site that mediate network-wide effects of DBS. Additionally, diffusion MRI can also characterize white matter tracts adjacent to the STN, such as the medial forebrain bundle, which

may also be important mediators of adverse events (Coenen *et al.*, 2009, 2012). Motor networks associated with clinically-effective STN-DBS have previously been delineated with diffusion MRI (Accolla *et al.*, 2016; Vanegas-Arroyave *et al.*, 2016; Akram *et al.*, 2017; Horn *et al.*, 2017; Chen *et al.*, 2018) but neuropsychiatric symptoms have not yet been comprehensively examined.

Using a high-resolution preoperative diffusion MRI acquisition, we reconstructed the distribution of subthalamic stimulation and its connectivity based on two frontostriatal networks recently shown to underlie dissociable aspects of impulsivity and gambling behaviour in patients with Parkinson's disease prior to STN-DBS (Mosley *et al.*, 2019*a*). These networks were chosen because of their involvement in cognitive mechanisms of central relevance for impulsivity: reward evaluation (sensitivity to appetitive rewards) and response inhibition (failure to suppress inappropriate or premature choices). Multiple lines of evidence implicate separable anatomical substrates of these 'choosing' and 'stopping' behaviours (Aron *et al.*, 2007; Haber and Knutson, 2010; van Eimeren *et al.*, 2010; Antonelli *et al.*, 2014; Rae *et al.*, 2015; Hampton *et al.*, 2017). In our previous study of patients with Parkinson's disease, we demonstrated brain-behaviour covariation between impulsivity and connectivity of these frontostriatal networks, with the effect of connectivity showing a distinction by ICB status. Here, we sought to identify the most important contributors to impulsivity after STN-DBS, examining the connectivity of frontostriatal networks prior to DBS and the connectivity of the stimulation field within these networks after DBS.

Materials and methods

Participants

Participants were consecutively recruited at the Asia-Pacific Centre for Neuromodulation in Brisbane, Australia between 2016 and 2018. All participants met the UK Brain Bank criteria for Parkinson's disease (Hughes *et al.*, 1992) and at the time of recruitment were being assessed for subthalamic DBS. All participants were at Hoehn and Yahr stage 2 or greater (Hoehn and Yahr, 1967) with motor fluctuations or other motor complications related to dopaminergic therapy. No participants met the Movement Disorder Society criteria for dementia (Emre *et al.*, 2007). The disease subtype was established based on an analysis of the dominant symptoms elicited during the Unified Parkinson's Disease Rating Scale (UPDRS) Part III Motor Examination, as described in Spiegel *et al.* (2007).

In the present longitudinal investigation, clinical and phenotypic assessments took place at baseline, prior to DBS (ON medication), and 3 months postoperatively (on stimulation). With presurgical results already reported (Mosley *et al.*, 2019*a*) the present report focuses on postoperative behaviours. However, preoperative findings are necessarily referenced when correlations between pre- and postoperative behaviours are analysed.

Ethics approval

Prior to the commencement of data collection, the full protocol was approved by the Human Research Ethics Committees of the Royal Brisbane and Women's Hospital, the University of Queensland, the QIMR Berghofer Medical Research Institute and UnitingCare Health. All participants gave written, informed consent to participate in the study.

Image acquisition

A preoperative T_1-weighted MPRAGE, a T_2-weighted FLAIR sequence and diffusion-weighted imaging (DWI) were obtained at baseline, using a 3 T Siemens Prisma and a 64-channel head coil. The acquisition parameters were as follows: T_1, 1 mm^3 voxel resolution, repetition time = 2000 ms, echo time = 2.38 ms, flip angle = 9°, matrix size = 256 × 256, field of view = 256 × 256 × 192; T_2, 1 × 1 × 2 mm voxel resolution, repetition time = 9500 ms, echo time = 122.0 ms, flip angle = 120°, matrix size = 256 × 256, field of view = 256 × 256 × 70; DWI, 90 directions, b-value = 3000 s/mm^2, voxel size = 1.7 mm^3 isotropic. Twelve non-diffusion-weighted images (b0) were interleaved throughout this main sequence, while an additional sequence of 8 b0 images were also acquired with the opposite phase-encoding (posterior-anterior) direction to allow for distortion correction. Postoperative CT images for all participants were acquired on a Siemens Intevo, with a resolution of 0.5 mm^3.

The DWI data were preprocessed with MRtrix3 (https://github.com/MRtrix3/mrtrix3), using an in-house preprocessing pipeline (https://github.com/breakspear/diffusion-pipeline). Preprocessing steps were identical to (Mosley *et al.*, 2019*a*). Full details on DWI acquisition, preprocessing and fibre reconstruction are provided in the Supplementary material.

Surgery and follow-up

After the STN was manually identified on FLAIR imaging, bilateral implantation of Medtronic 3389, Boston Vercise or Abbott 6172 directional electrodes took place in a single-stage procedure using a Leksell stereotactic apparatus. Intraoperative microelectrode recordings (MERs) were used to identify the boundaries of the STN and intraoperative test stimulation was performed. Postoperative lead placement was confirmed with CT imaging. Subthalamic stimulation was commenced immediately with the initial choice of contact based upon MER signals. After discharge, participants returned to the clinic at set intervals for further titration of stimulation (including changes in stimulating contact) against motor symptoms until these were satisfactorily treated without adverse effects. Dopaminergic medication was reduced or ceased postoperatively, with remaining treatment converted to a levodopa-equivalent daily dose (LEDD) value (Evans *et al.*, 2004).

Assessment of impulsivity

All participants were assessed for impulsivity at baseline and at follow-up, 3 months after DBS surgery. Participants were phenotyped on both occasions using a combination of neuropsychiatric instruments and engagement in a naturalistic gambling paradigm (the 'virtual casino').

Neuropsychiatric instruments

Impulsivity was assessed with a range of neuropsychiatric instruments, to account for the multidimensional nature of this construct (Mosley *et al.*, 2019*a*). These included: trait

impulsiveness: the Barratt Impulsiveness Scale 11 (BIS) (Patton *et al.*, 1995); impulsive and compulsive behaviours (ICBs): the Questionnaire for Impulsive-Compulsive Disorders in Parkinson's Disease-Rating Scale (QUIP-RS) (Weintraub *et al.*, 2012); impatience: the Delay Discounting Task (Kirby *et al.*, 1999); disinhibition: the Excluded Letter Fluency task (ELF) (Shores *et al.*, 2006) and the Hayling test (Burgess and Shallice, 1997). In addition, depressive symptoms were assessed with the Beck Depression Inventory (Beck *et al.*, 1961) and apathetic symptoms with the Apathy Scale (Starkstein *et al.*, 1992). To assess basic cognitive status, the Mini-Mental State Examination (MMSE) (Folstein *et al.*, 1975) and the Montreal Cognitive Assessment (MoCA) (Nasreddine *et al.*, 2005) were also administered. For further information, see the Supplementary material. Statistical analyses of differences in impulsivity between pre- and post-DBS assessments were corrected for multiple comparisons using the Benjamini and Hochberg method (1995), with $\alpha = 0.05$.

Gambling paradigm

Participants gambled on slot machines within a virtual casino (Supplementary Fig. 1) that has previously been used to study impulsive decision-making in healthy controls and patients with Parkinson's disease (Paliwal *et al.*, 2014, 2019). This naturalistic gambling task allowed for impulsive behaviour to be expressed as bet increases, exploratory slot machine switches and 'double or nothing' gambles. Full details of this task are given in Mosley *et al.* (2019*a*), Paliwal *et al.* (2019) and the Supplementary material.

Caseness

Following DBS surgery, in addition to the dimensional assessment of impulsivity and gambling behaviour, participants were also assigned to the category 'case' or 'non-case' depending on whether they developed clinically-significant (i.e. impairment or distress) neuropsychiatric symptoms attributable to DBS, necessitating device manipulation (hereafter referred to as 'caseness'). Identification of these patients used the same process as prior work (Mosley *et al.*, 2018*a*, *c*, 2019*b*). This category was operationalized as follows: participants were evaluated at baseline and postoperatively by a neuropsychiatrist (P.M.). A semi-structured diagnostic interview and mental state examination were undertaken with attention to euphoria, irritability, disinhibition, impulsivity and compulsivity. The contribution of neurostimulation to the presentation was confirmed if symptoms responded promptly to a reduction in the amplitude or change in the locus of stimulation, as assessed by serial mental state examinations and feedback from close family members. Clinically-significant neuropsychiatric symptoms had remitted in all participants by the time of the postoperative reassessment of impulsivity and gambling.

Electrode localization and volume of tissue activation

DBS electrodes were localized using the Lead-DBS toolbox version 2.2 (Horn and Kuhn, 2015; Horn *et al.*, 2019*a*) (https://github.com/netstim/leaddbs/tree/develop). Preoperative structural acquisitions were co-registered with postoperative CT imaging and then normalized into common ICBM 2009b non-linear asymmetric space using the SyN approach implemented in advanced normalization tools (ANTs) (Avants *et al.*, 2008). Electrode trajectories were reconstructed after correcting for brainshift in postoperative acquisitions by applying a refined affine transform in a subcortical area of interest calculated pre- and postoperatively. Rotation of directional electrodes was determined based on visualization of the artefact created by the orientation marker and directional electrode segments (Hellerbach *et al.*, 2018). For each electrode, a volume of activated tissue (VAT) was estimated using a volume conductor model of the DBS electrode and surrounding tissue, based on each participant's individualized stimulation settings and a finite element method to derive the gradient of the potential distribution (Horn *et al.*, 2019*a*). An electric field (E-field) distribution was also modelled (Vorwerk *et al.*, 2018).

Tractography and apparent fibre density

Using the preoperative DWI data, constrained spherical deconvolution (CSD) (Tournier *et al.*, 2004, 2007; Jeurissen *et al.*, 2014) was performed in each participant after group-average intensity normalization (Raffelt *et al.*, 2012), generating voxel-wise estimates of fibre orientation distribution functions (fODF). Fibre tracts from seed (subcortical) to target (cortical) regions were reconstructed with the probabilistic streamline algorithm iFOD2 (Tournier *et al.*, 2010). Estimates of structural connectivity between each seed and target region were derived from the apparent fibre density representing the underlying intra-axonal volume averaged along tracts (Raffelt *et al.*, 2012) (Supplementary Fig. 2 and Supplementary material).

Networks

The influence of the site and distribution of stimulation on postoperative impulsivity and gambling was evaluated using two discrete brain networks supporting reward evaluation and response inhibition (Fig. 1A). These networks incorporate anatomical priors, as below. We chose to employ the same networks used in Mosley *et al.* (2019*a*), which were found to explain a substantial fraction of the variance in impulsivity prior to DBS. We defined these networks at baseline, prior to STN-DBS, and adjust their anatomical features postoperatively to incorporate the subthalamic VAT as the seed for probabilistic tractography.

The preoperative reward evaluation network comprised streamlines connecting ventral striatum with anterior cingulate cortex, orbitofrontal cortex (OFC), ventromedial prefrontal cortex (vmPFC) and the ventral tegmental area (VTA), as well as the STN with vmPFC. The preoperative response inhibition network connected the STN with the inferior frontal gyrus (IFG) and pre-supplementary motor area (SMA). Although other cortical areas (such as the anterior cingulate cortex) are implicated in cognitive control, we focused on the IFG and SMA because of the strong empirical support for this network in prior work on behavioural inhibition (Rae *et al.*, 2015; Hughes *et al.*, 2018). These baseline networks were used to evaluate the influence of structural connectivity prior to DBS on postoperative impulsivity and gambling. Postoperatively, these networks were extended to incorporate the subthalamic VAT, with a focus on connections of the VAT within the network. The reward evaluation network now included streamlines connecting the site of stimulation with OFC, vmPFC, ventral striatum and VTA. To capture tegmental

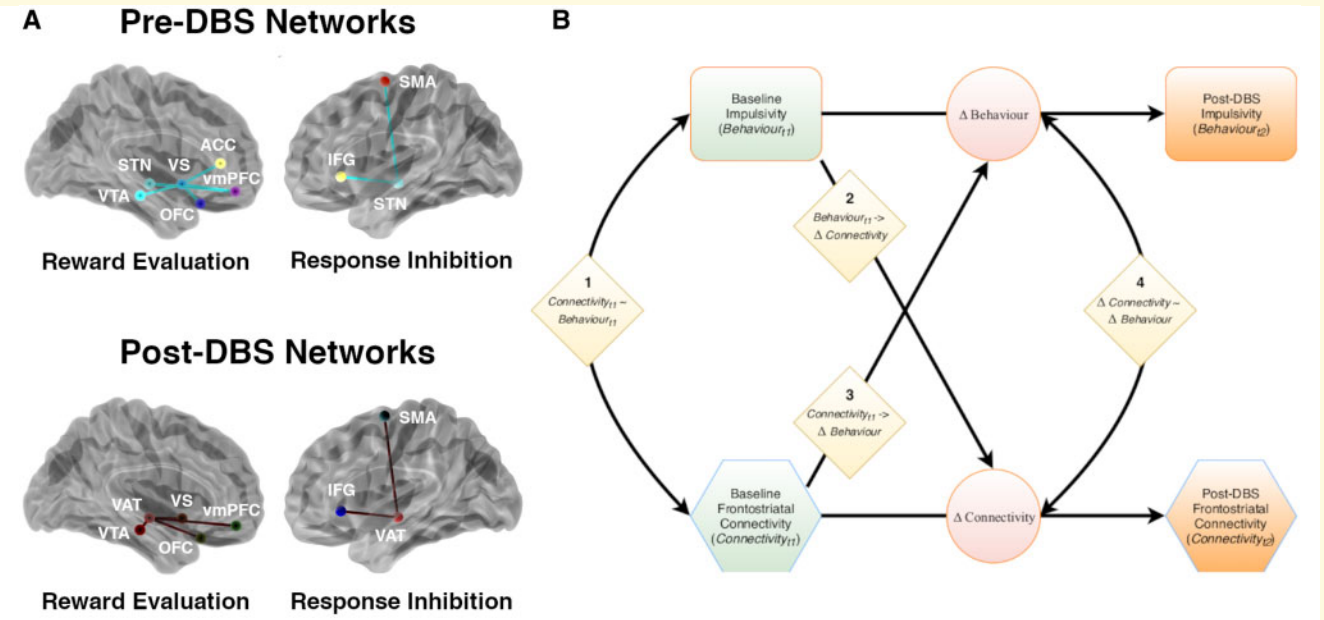

Figure 1 Modelling brain-behaviour covariation. (**A**) Two discrete networks subserving reward evaluation and response inhibition were specified based on Mosley *et al.* (2019*a*). The pre-DBS reward evaluation network was defined to include tracts connecting ventral striatum (VS) with vmPFC, OFC, anterior cingulate cortex (ACC) and VTA. It also included a tract connecting the STN with vmPFC. The response inhibition network included tracts connecting the STN with the IFG and the SMA. Postoperatively, these networks were extended to incorporate the subthalamic VAT, with a focus on connections of the VAT within the network. Network models were visualized with the BrainNet Viewer (Xia *et al.*, 2013). (**B**) Cross lagged (latent change score) model which allows quantification of the relationship between preoperative structural network connectivity (Connectivity$_{t1}$) and baseline measures of impulsivity (Behaviour$_{t1}$) to post-DBS structural network connectivity (Connectivity$_{t2}$) and postoperative measures of impulsivity (Behaviour$_{t2}$). Coefficients are modelled as follows: 1, connectivity-behaviour covariance at baseline (Connectivity$_{t1}$ ~ Behaviour$_{t1}$); 2, behaviour to connectivity coupling (Behaviour$_{t1}$ → ΔConnectivity); 3, connectivity to behaviour coupling (Connectivity$_{t1}$ → ΔBehaviour); and 4, an estimate of correlated change in connectivity and behaviour (ΔConnectivity ~ ΔBehaviour). In the context of the present investigation, we were mainly interested in connectivity to behaviour coupling (3). Diamonds = coefficients; circles = change scores; rectangles = measured indices of impulsivity; hexagons = structural connectivity profiles. For these latter two variables, green shading indicates preoperative data and orange shading indicates postoperative data. See the main text and Supplementary material for further elaboration of these relationships. LEDD = levodopa equivalent daily dose; PCA = principal components analysis.

fibres for this latter midbrain region, the VTA served as the seed and the subthalamic VAT as the target. The response inhibition network included tracts connecting the VAT with IFG and SMA.

Further details of these parcellations are provided in the Supplementary material.

Data analysis

Partial least squares path modelling

Partial least squares path modelling (PLS-PM) was used to identify specific patterns of structural connectivity explaining inter-individual variability in impulsivity and gambling behaviour after STN-DBS (McIntosh and Lobaugh, 2004; Shaw *et al.*, 2016), controlling for relevant demographic and disease-related factors (Supplementary Fig. 3). PLS-PM is a method for examining a system of linear relationships between multiple blocks of variables. In this investigation, we were interested in how brain structure (connectivity) affected impulsivity (behaviour) and whether this was also influenced by age, gender, duration of disease, subtype of disease and dopaminergic medication. The connectivity variable in the path model was constructed from the apparent fibre density of each white matter tract in the structural network under investigation. The individual contribution of each tract to the connectivity variable was quantified by a 'weight' (linear coefficient) and the connectivity variable was formed as a linear mixture of the corresponding apparent fibre density values that most strongly covaried with the behavioural variable under investigation. The relationship between the connectivity and behavioural variables was quantified in the path model by a path coefficient and tested for statistical significance using bootstrapping. Relevant demographic and disease-related covariates were also represented and path coefficients were determined for these relationships. Bootstrapping of the model yielded 95% confidence intervals for the coefficients of interest.

All models were constrained to be of equivalent complexity: each model used either the reward evaluation or the response inhibition network, plus LEDD, age and years since diagnosis of Parkinson's disease. One interaction term (e.g. the interaction of LEDD with the reward evaluation network) was permitted per model and reported if significant. The winning model from all possible permutations (network, interaction effect if significant) was selected based on the maximum R^2 value prior to bootstrapping, which was used as the summary metric to compare models. The influence of gender, disease-subtype, pre-DBS ICB

status and post-DBS caseness on the association between connectivity and behaviour was examined with a permutation test in the PLS path model, performed upon the winning model for each behavioural variable of interest. For further details, see the Supplementary material.

Longitudinal modelling

Using the weighted network scores derived from PLS-PM, with pre- and post-DBS behavioural evaluations, a cross-lagged panel model was used to evaluate whether structural connectivity at baseline ($Connectivity_{t1}$) influenced impulsivity and gambling postoperatively ($Behaviour_{t2}$) (Fig. 1B). These latent change score models assess longitudinal associations between two or more repeatedly sampled measures of brain and behaviour (Kievit *et al.*, 2018; Muetzel *et al.*, 2018; Lin *et al.*, 2019). They quantify cross-domain coupling, capturing the extent to which change (Δ) in one domain (impulsivity) reflects the baseline level in the other (connectivity) and vice versa. Here, a bivariate cross-lagged model described four brain-behaviour relations of interest. These comprised connectivity-behaviour covariance at baseline ($Connectivity_{t1} \sim Behaviour_{t1}$), connectivity to behaviour coupling ($Connectivity_{t1} \rightarrow \Delta Behaviour$), behaviour to connectivity coupling ($Behaviour_{t1} \rightarrow \Delta Connectivity$) and an estimate of correlated change in connectivity and behaviour ($\Delta Connectivity \sim \Delta Behaviour$) after taking into account the coupling pathways. Change in connectivity (ΔConnectivity) was defined as the change in network connectivity after the subthalamic VAT was added as a seed for probabilistic tractography. In the context of the present investigation, we were mainly interested in the ability of pre-DBS network connectivity to predict cognitive change from pre- to post-DBS ($Connectivity_{t1} \rightarrow \Delta Behaviour$). Model fit metrics comprised the Comparative Fit Index (CFI; the degree to which the proposed model better fits the data than one that assumes no correlations amongst latent variables) and the root mean square error of approximation (RMSEA; a measure of the deviation between observed covariance and that predicted by the model). Notably, we omitted longitudinal modelling of demographic and disease-related covariates in these latent change score models and focused only on the longitudinal coupling of brain connectivity and behaviour. We did this for two reasons: (i) our goal was to test a relatively straightforward baseline assay (brain connectivity) of vulnerability to postoperative impulsivity, which could be implemented in clinical practice without excessively complex statistical methods; and (ii) building a cross-lagged model that represents all conceivable covariates is a difficult task, possibly leading to excessively complex models (Kievit *et al.*, 2018). Unless a clear role for covariates was identified in the PLS path models, we opted for a more parsimonious representation.

For the gambling outcomes, random-intercept linear mixed-effects models were fit in order to provide an explicit longitudinal metric of change (e.g. in dollars wagered) by connectivity (Supplementary material).

Caseness

Supplementary analyses were undertaken to explore distinct patterns of connectivity in individuals with clinically-significant, stimulation-dependent neuropsychiatric symptoms ('cases') based on their betting behaviour (Fig. 2). This required co-registration of individual participant data with a common anatomical reference. To achieve this, using the Lead-DBS toolbox, each participant's VAT in each hemisphere was integrated with a normative structural connectome derived from 90 patients with Parkinson's disease (mean age 61.4 ± 10.4, 28 females) enrolled in the Parkinson's Progression Markers Initiative (PPMI, www.ppmi-info.org), in which 20 000 fibres were sampled per subject using a generalized q-sampling approach implemented in DSI-Studio (Yeh *et al.*, 2010), as described in more detail in Ewert *et al.* (2018) and Horn *et al.* (2017). Fibres traversing each participant's VAT were selected from the group connectome based on the E-field gradient strength (i.e. fibres in peripheral VAT regions with a low E-field were down-weighted) and projected to the volumetric surface of the ICBM 2009b non-linear asymmetric brain in 1 mm isotropic resolution. A connectivity profile for each participant was expressed as the weighted number of fibre tracts between the stimulation site and each brain voxel. Subsequently, to visualize subcortical streamlines predictive of outcome, all fibres traversing VATs across the cohort were isolated from the normative connectome.

Discriminating by caseness, fibres associated with bet size in the virtual casino were identified. Each fibre was tested across the cohort between participants with a stimulation volume that encompassed the fibre (connected) and those where the fibre did not traverse the volume (unconnected). If there was a significant difference between betting behaviour in participants with connected and unconnected VATs (using a two-sided, two-sample *t*-test), then this fibre was identified as discriminative of outcome. This process yielded a 'fibre *t*-score', with high-values indicating that this fibre was strongly discriminative of clinical outcome (Baldermann *et al.*, 2019). Only the top 20% of fibres positively correlated with the behavioural variable were selected for analysis to mitigate the risk of false positive associations.

Focal subthalamic stimulation

Supplementary analyses were also undertaken to investigate the effects of focal stimulation within the STN on motor and neuropsychiatric outcomes. The spatial position of each electrode contact and the distribution of each VAT was evaluated with reference to a multimodal parcellation of the STN into affective, associative and motor subregions (Ewert *et al.*, 2018). For each hemisphere, the following variables were calculated: (i) the distance of the active electrode contact to the centroid of each STN subregion; and (ii) the extent of each subregion volume occupied by each participant's VAT (i.e. representing the dispersion of charge).

To reduce the dimensionality of this dataset, as with Mosley *et al.* (2018*c*), a variable selection and regularization algorithm (the Least Absolute Shrinkage and Selection Operator: LASSO) was used to identify the combination of anatomical variables with the best predictive value for each neuropsychiatric outcome (Friedman *et al.*, 2010). A conservative one-standard-deviation rule was chosen for the regularization parameter (λ) to protect against overfitting (Hastie *et al.*, 2009).

Subsequently, neuropsychiatric variables and their anatomical predictors as identified from the LASSO were modelled in a general linear model. Demographic and disease-related factors, including LEDD, were also entered as covariates.

Data and code availability

Data analysis was performed in the R software environment (R Core Team, 2014), using the packages *glmnet* for optimization (Friedman *et al.*, 2010), *plspm* for PLS-PM (Sanchez, 2013), *pls* for PLS regression (Mevik, 2007), *lavaan* for cross-lagged

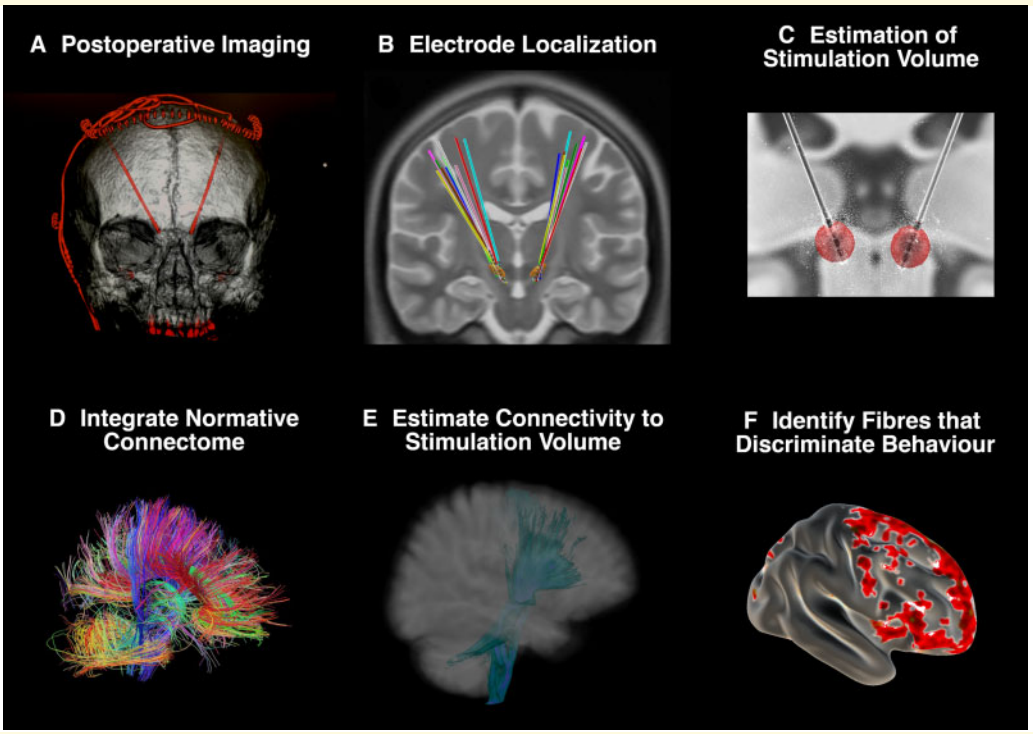

Figure 2 Identifying fibres discriminative of gambling behaviour. A supplementary analysis was undertaken to identify distinct patterns of connectivity between 'cases' and 'non-cases'. (**A**) Subthalamic electrodes were identified on postoperative imaging. (**B**) Electrodes were localized in ICBM 2009b non-linear asymmetric space using the Lead-DBS toolbox. (**C**) Stimulation volumes were estimated for each participant based on individual stimulation parameters. (**D**) A normative connectome from the PPMI was integrated with the cohort. (**E**) Fibres from this connectome passing through each stimulation volume were isolated. (**F**) Measuring the behavioural variable (bet size in the virtual casino), each fibre was tested across the cohort between participants with a stimulation volume that encompassed the fibre (connected) and those where the fibre did not traverse the volume (unconnected). If there was a significant difference in bet size between participants with connected and unconnected VATs, then this fibre was identified as associated with betting behaviour. The top 20% of discriminative fibres were compared between 'case' and 'non-case' groups to identify distinct patterns of connectivity.

models (Rosseel, 2012) and *lme4* for linear mixed-effects models (Bates *et al.*, 2015).

The gambling paradigm is provided for download from a git repository at https://github.com/saeepaliwal/breakspear_slot_machine and the analysis pipeline at https://github.com/saeepaliwal/dbs_pd_analysis_pipeline. The diffusion MRI processing pipeline is at https://github.com/breakspear/diffusion-pipeline. Code for the analysis of focal STN stimulation is at https://github.com/AlistairPerry/DBSVATstats. A de-identified dataset containing neuropsychiatric assessment and gambling data can be provided on application to the corresponding author, subject to institutional review board approval.

Results

Participants

Fifty-seven surgical candidates gave informed consent and completed all baseline assessments. Two participants were unable to complete the postoperative assessments because of fatigue. Fifty-five participants thus proceeded to analysis (Table 1). Prior to surgery, 17 participants had a current or past history of an ICB and six participants had more than one ICB. These all developed after the diagnosis of Parkinson's disease and in the setting of dopaminergic therapy (including both levodopa and dopamine agonist treatment). These comprised pathological gambling ($n = 10$), hypersexuality ($n = 9$), compulsive shopping ($n = 3$), dopamine dysregulation ($n = 2$), binge eating ($n = 1$) and hobbyism ($n = 1$). Participants with ICBs were more likely to be male [$\chi^2(1) = 7.20$, corrected $P = 0.044$] and younger ($t = 2.78$, mean difference 8.6 years, corrected $P = 0.044$). Implanted devices comprised Medtronic 3389 ($n = 21$), Boston Scientific Vercise ($n = 18$) and Abbott 6172 directional electrodes ($n = 16$). Directional electrodes were used in five participants to steer current. Across all participants, subthalamic VATs in each hemisphere were concatenated, with the highest probability of stimulation occurring in the dorsolateral aspect of the STN in both hemispheres [Fig. 3A(i and ii)].

Postoperatively, there was a significant decrease in UPDRS part III motor examination score ($t = 3.80$, mean difference 6.6 points, corrected $P = 0.0020$) and levodopa equivalent daily dose ($t = 9.68$, mean difference 746 mg, corrected

$P = 2.1 \times 10^{-13}$). At a group level, there was also a significant decrease in disinhibition as assessed by the Hayling AB Error Score ($t = 2.60$, mean difference 4.2 points, corrected $P = 0.044$). There were no other significant pre-post group differences amongst the neuropsychiatric instruments assessing impulsivity or gambling behaviours (Table 1). Only 17 participants used the machine switch option in the virtual casino and this measure was hence not analysed further. There were no significant changes in cognition, depressive or apathetic symptoms across the cohort. One participant developed clinically-significant depressive symptoms and these were treated with an antidepressant. Seventeen participants developed a postoperative elevation in mood and clinically-significant impulsive behaviour attributable to stimulation ('cases'; specific neuropsychiatric symptoms are detailed in Supplementary Table 1). Clinically significant psychiatric symptoms had remitted in these individuals at the time of postoperative assessment (device manipulations used to remit symptoms are detailed in Supplementary Table 2). Subthalamic VATs were compared amongst cases before and after remission of symptoms [Fig. 3B(i and ii)]. There was a qualitative trend for stimulation associated with acute symptoms to be located in more ventromedial aspects of the nucleus, with remission of symptoms associated with more dorsolateral stimulation (*cf.* red and green concatenated fields of overlapping voxels). Between case-positive and case-negative participants, there were no significant differences in dimensional variability amongst neuropsychiatric indices of impulsivity derived from the clinical assessments or gambling behaviours derived from the virtual casino (Supplementary Table 3). A history of current or past ICBs was not predictive of developing a neuropsychiatric syndrome post-DBS [$\chi^2(1) = 0.62$, $P = 0.43$]. Participants with a history of ICBs prior to surgery also did not differ in

Table 1 Demographic and clinical characteristics of the Parkinson's disease cohort ($n = 55$)

Demographic and disease-related variables			
Categorical variable	**Total ($n = 55$)**	**Percentage total**	
Gender	*n*	% total	
Male	36	65.5	
Female	19	34.5	
Clinical subtype	*n*	% total	
Akinetic-rigid	17	30.9	
Mixed	27	49.1	
Tremor	11	20.0	
ICB status	*n*	% total	
Yes	17	30.9	
No	38	69.1	
Continuous variable	**Mean (SD), median [range]**		
Age, years	62.0 (±9.8), 65 [35–77]		
Hoehn and Yahr stage	2.6 (±0.5), 2.5 [1.5–4]		
Years since diagnosis	8.2 (±4.2), 7 [2–21]		
Variables assessed pre- and post-DBS, mean (SD), median [range]			
Assessment instrument	**Pre-DBS**	**Post-DBS**	**Pre- versus post-DBS[a]**
LEDD	1126 (±629.9), 1015 [0–3450]	380 (±231.4), 375 [0–825]	$t = 9.68$; *corr.* $P = 2.1 \times 10^{-13}$***
BIS Attentional	16.0 (±3.4), 16 [10–26]	15.5 (±4.3), 15 [8–31]	$t = 1.40$; *corr.* $P = 0.25$
BIS Non-Planning	22.6 (±4.1), 23 [14–32]	22.7 (±5.3), 22 [14–37]	$t = -0.14$; *corr.* $P = 0.92$
BIS Motor	21.5 (±3.7), 21 [14–30]	20.7 (±3.8), 21 [13–34]	$t = 1.99$; *corr.* $P = 0.11$
QUIP-RS Total	20.0 (±15.3), 18 [0–63]	18.6 (±16.6), 15 [0–66]	$t = 0.80$; *corr.* $P = 0.53$
Delay discount, *k*	0.038 (±0.064), 0.016 [0.00016–0.25]	0.028 (±0.031), 0.016 [0.00016–0.1]	$t = 1.59$; *corr.* $P = 0.19$
Hayling AB Error Score	14.2 (±13.1), 9 [0–44]	10.0 (±10.6), 5 [0–39]	$t = 2.60$; *corr.* $P = 0.044$*
ELF Rule Violations	8.6 (±5.4), 8 [0–24]	7.1 (±4.7), 6 [1–22]	$t = 2.29$; *corr.* $P = 0.072$
Beck Depression Inventory	11.0 (±5.1), 10 [2–24]	9.3 (±8.3), 8 [0–44]	$t = 1.84$; *corr.* $P = 0.14$
Apathy Scale	12.0 (±4.8), 11 [2–26]	12.3 (±5.4), 11 [3–29]	$t = -0.50$; *corr.* $P = 0.83$
MMSE	28.3 (±1.5), 28 [25–30]	28.3 (±2.5), 29 [27–30]	$t = 0.20$; *corr.* $P = 0.84$
MoCA	26.0 (±2.3), 26 [21–30]	26.6 (±3.0), 28 [15–30]	$t = -1.95$; *corr.* $P = 0.14$
UPDRS Part III Motor	39.4 (±15.1), 39 [10–70]	32.9 (±13.0), 32 [8–60]	$t = 3.80$; *corr.* $P = 0.0020$**
Virtual casino			
Average bet size (AUD)	42.2 (±45.2), 27.2 [5–191.8]	61.4 (±78.0), 25.7 [5–339.8]	$t = -1.87$; *corr.* $P = 0.12$
Double or nothing gamble, %	17.1 (±20.7), 15 [0–100]	17.4 (±20.1), 19 [0–100]	$t = -0.097$; *corr.* $P = 0.92$

[a]FDR-corrected with Benjamini and Hochberg method (1995), with $\alpha = 0.05$.
Significance: *$P < 0.05$; **$P < 0.01$; ***$P < 0.001$.
BIS = Barratt Impulsiveness Scale; ELF = Excluded Letter Fluency Task; LEDD = levodopa equivalent daily dose; MMSE = Mini Mental State Examination; MoCA = Montreal Cognitive Assessment; QUIP-RS = Questionnaire for Impulsive-Compulsive disorders in Parkinson's Disease-Rating Scale; UPDRS = Unified Parkinson's Disease Rating Scale Part III Motor Examination.

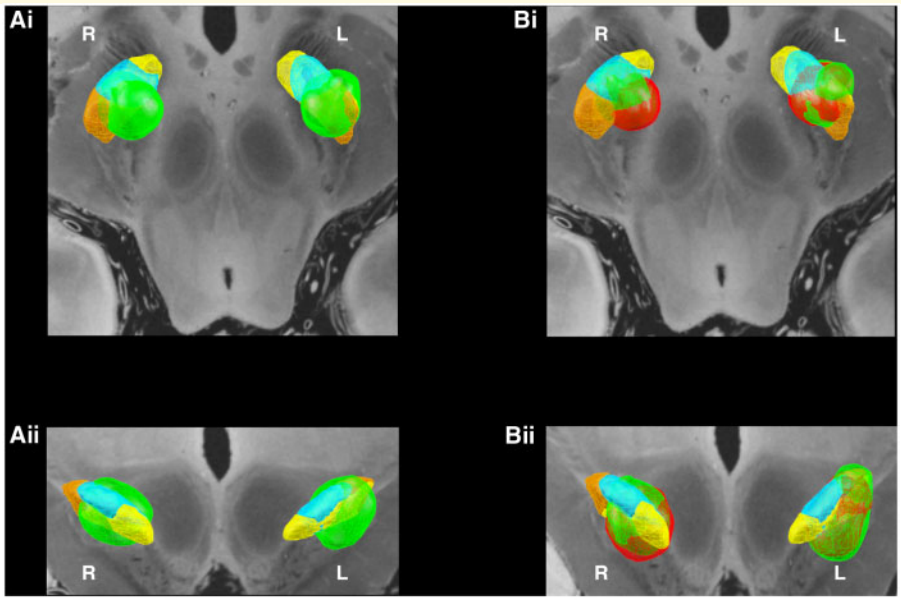

Figure 3 Subthalamic stimulation. VATs for each participant in each hemisphere were concatenated and thresholded to identify the highest frequency of overlapping voxels (the top 25% are shown here). The VATs overlapped most substantially with the dorsolateral aspects of the STN in both hemispheres. The subthalamic atlas (Ewert *et al.*, 2018) is overlaid on a 7 T MRI *ex vivo* brain image (Edlow *et al.*, 2019). Within each STN, affective = yellow, associative = blue, and motor = maroon subregions. [**A**(**i** and **ii**)] Axial and coronal visualizations of stimulation across the whole cohort (green). [**B**(**i** and **ii**)] For those participants who developed clinically-significant neuropsychiatric symptoms (cases), the VATs are visualized at the time of symptom onset (red) and after stimulation manipulation (reduction in amplitude, change of contact etc.) when acute symptoms had resolved (green). A qualitative trend away from ventromedial regions can be seen after stimulation adjustment associated with remission of neuropsychiatric symptoms.

postoperative neuropsychiatric measures or gambling behaviours (Supplementary Table 3).

Path modelling of connectivity and impulsivity

Overview

Impulsivity was assessed using either neuropsychiatric instruments or gambling behaviours in a virtual casino. The variance in impulsivity explained by the structural connectivity of the subthalamic VAT was estimated using PLS path models. The variance explained by frontostriatal connectivity was higher for betting behaviour in the virtual casino, than for the neuropsychiatric instruments. Employing a cross-lagged model, postoperative changes in impulsivity and gambling were not significantly related to the structural connectivity of frontostriatal networks at baseline, prior to DBS. Finally, the effect of connectivity on bet size in the virtual casino differed amongst participants who developed postoperative, stimulation-dependent neuropsychiatric symptoms characterized by mood elevation, irritability, disinhibition and impulsivity reaching the threshold of clinical-significance (cases).

Barratt Impulsiveness Scale

We first examined how self-reported impulsiveness after DBS was related to the structural connectivity of networks incorporating the participant-specific stimulation field at each DBS electrode. The connectivity of the response inhibition network best explained variations in this construct. The greater the connectivity of the VAT with the response inhibition network, the greater the impulsiveness (coefficient = 0.36, $P = 0.010$; Table 2). The tracts weighted most heavily in the response inhibition network linked the VAT with left SMA and right IFG (Fig. 4A and Supplementary Table 4). There was no significant difference by preoperative ICB status ($P = 0.57$) or postoperative caseness ($P = 0.33$) on this effect. The connectivity of the VAT with the response inhibition network explained 15.4% of the total postoperative variance in impulsiveness.

We next used a cross-lagged model to assess the contribution of structural connectivity at baseline to postoperative changes in impulsiveness. This postoperative change was not significantly influenced by the structural connectivity of the response inhibition network prior to DBS ($P = 0.071$; Table 3). However, there was a significant cross-sectional association prior to DBS between impulsiveness and connectivity (coefficient = –2.38, $P = 0.017$), with greater connectivity of this network linked to reduced impulsivity in this domain, the opposite of the post-DBS effect (compare the sign of the coefficient in the PLS path model above). There was also a significant correlated change in connectivity and impulsivity from the pre- to the postoperative interval (coefficient 1.74,

$P = 0.023$), suggesting a co-occurrence of connectivity and behavioural changes (Supplementary Fig. 4).

Questionnaire for Impulsive-Compulsive Disorders in Parkinson's Disease-Rating Scale

There were no significant associations between dimensional ratings of behavioural addictions (such as gambling, sex, shopping and eating) and structural connectivity with the site of stimulation, either within the response inhibition or reward evaluation network.

Excluded Letter Fluency rule violations

We then evaluated how structural connectivity with the site of stimulation was related to postoperative disinhibition (as expressed by ELF rule violations). The connectivity of the reward evaluation network best explained variability in this facet of impulsivity. The greater the connectivity of the VAT with the reward evaluation network, the more inhibitory errors (coefficient = 0.41, $P = 0.0017$; Table 2). The tract weighted most heavily in the reward evaluation network linked the VAT with right vmPFC (Fig. 4B and Supplementary Table 5). There was no significant difference by preoperative ICB status ($P = 0.62$) or postoperative caseness ($P = 0.78$) on the effect of connectivity. The connectivity of the VAT with the reward evaluation network explained 16.9% of the total postoperative variance in disinhibition.

In the cross-lagged model, there was no significant effect of baseline structural connectivity on postoperative changes in disinhibition ($P = 0.12$; Table 3). Again, prior to DBS there was a cross-sectional association between connectivity and disinhibition (coefficient = –0.51, $P = 0.018$), with greater connectivity in the reward evaluation network associated with fewer inhibitory errors, again the opposite of the post-DBS effect. There was also a significant co-occurrence of connectivity and behavioural changes after DBS (coefficient = 0.34, $P = 0.0050$) (Supplementary Fig. 5).

Hayling AB Error Score

The structural connectivity of networks incorporating the participant-specific stimulation field (both response inhibition and reward evaluation) did not associate with variation in disinhibition (as expressed by Hayling A or B errors).

Delay Discount *k*

Last amongst the neuropsychiatric instruments, we considered delay discounting: the tendency to prefer sooner, smaller rewards over those that are larger but temporally more distant. Postoperatively, behaviour on this task was best explained by the connectivity of the site of stimulation within the reward evaluation network. The greater the connectivity of the VAT with the reward evaluation network, the lower the impatience and the greater the ability to defer reward (coefficient = –0.31, $P = 0.042$; Table 2). The tracts weighted most strongly in the reward evaluation network were bi-hemispheric connections between the VTA and the site of stimulation (Fig. 4C and Supplementary Table 6). There was no significant difference by preoperative ICB status ($P = 0.15$) or postoperative caseness ($P = 0.14$) on the effect of connectivity. The connectivity of the VAT with the reward evaluation network explained 3.3% of the total postoperative variance in impatience.

Using the cross-lagged model, postoperative change in impatience was not influenced by the structural connectivity of the reward evaluation network prior to DBS ($P = 0.67$; Table 3). At baseline, there was significant connectivity-behaviour covariance (coefficient = –0.46, $P = 0.020$) with greater connectivity of the reward evaluation network also associated with a greater ability to defer reward. Connectivity and behavioural changes pre- to post-DBS were not significantly correlated ($P = 0.85$) (Supplementary Fig. 6).

Bet size

Inter-individual variation in bet size post-DBS in the virtual casino was best explained by the connectivity of the VAT with the reward evaluation network. The greater the connectivity of the VAT with the reward evaluation network, the higher the bets in the casino (coefficient = 0.43, $P = 0.0029$; Table 2). Tracts weighted most heavily were those linking the stimulation field with right and left OFC, right vmPFC and left ventral striatum (Fig. 4D and

Table 2 Detailed output of models from PLS-PM analysis of postoperative behaviour

PLS-PM analysis of post-DBS impulsivity and gambling						
Variable	**Network**	**R^2**	**Path coefficient**	**Significance *P*-value**	**95% CI**	**Other significant covariates**
Post-DBS neuropsychiatric instruments						
BIS	Response inhibition	0.19	0.36	0.010*	0.062 to 0.58	Nil
ELF rule violations	Reward evaluation	0.27	0.41	0.0017**	0.15 to 0.62	Nil
Delay Discount *k*	Reward evaluation	0.14	–0.31	0.042*	–1.00 to –0.049	Years since diagnosis: *coeff* = –0.33 95% CI = –0.55 to –0.092 *P* = 0.030
Post-DBS gambling behaviours						
Bet size	Reward evaluation	0.30	0.43	0.0029**	0.044 to 0.64	Nil

Significance: *$P < 0.05$; **$P < 0.01$; ***$P < 0.001$.

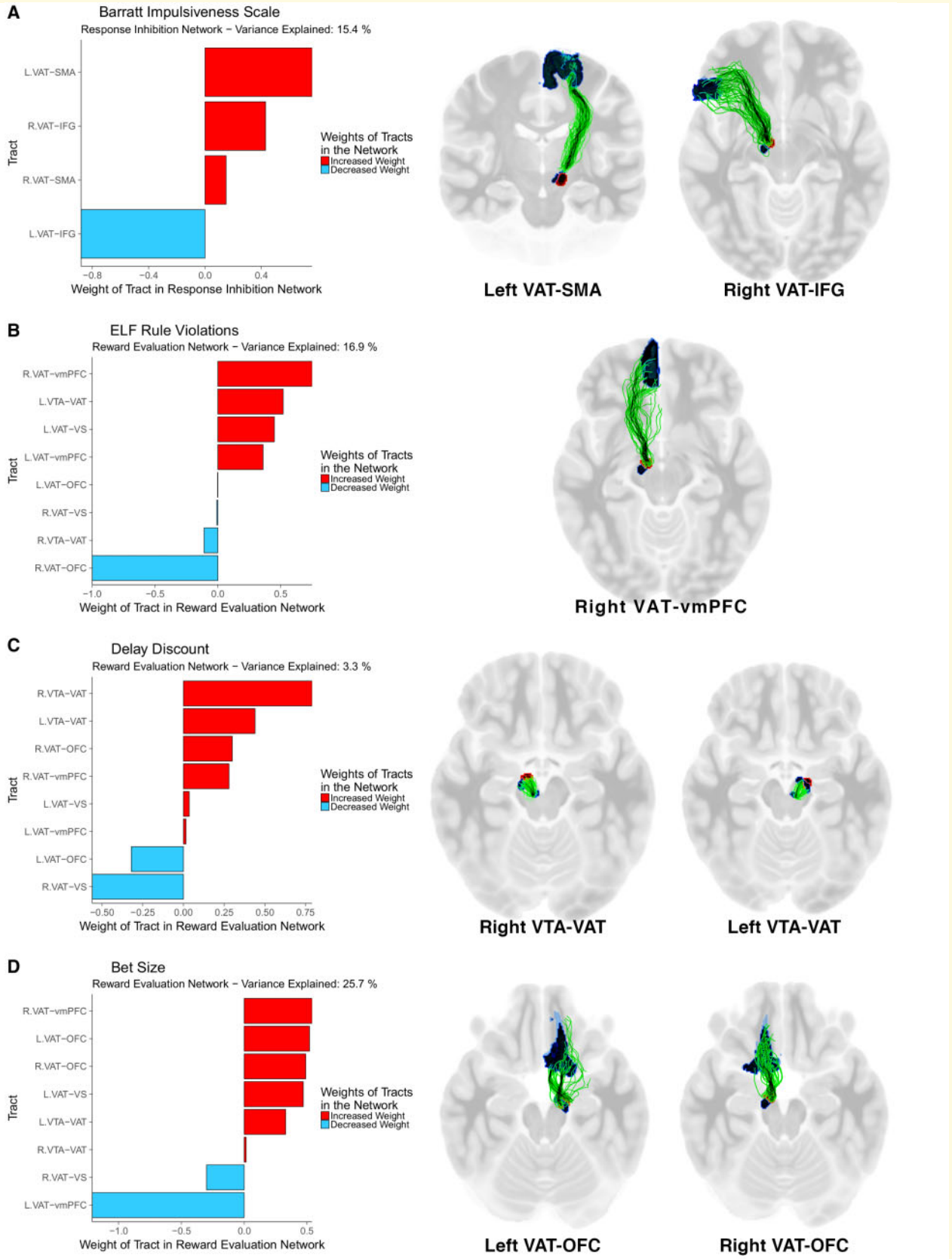

Figure 4 Fibre tracts weighted most strongly in the association of connectivity with impulsivity and gambling. The anatomical network with the greatest capacity to explain variance in each aspect of postoperative impulsivity and gambling. *Left column*: In each PLS path model, the anatomical variable representing structural connectivity was composed of a weighted mixture of all tracts in the network. *Right column*: The most heavily weighted tracts. (**A**) Barratt Impulsiveness Scale; (**B**) ELF rule violations; (**C**) Delay Discount constant k; (**D**) Bet size. VS = ventral striatum.

Table 3 Cross-lagged model results

Variable	Cross-lagged coefficients		Cross-sectional coefficients		Model fit indices	
	$Connectivity_{t1} \rightarrow \Delta Behaviour$	$Behaviour_{t1} \rightarrow \Delta Connectivity$	$Connectivity_{t1} \sim Behaviour_{t1}$	$\Delta Connectivity \sim \Delta Behaviour$	CFI	RMSEA
Post-DBS neuropsychiatric instruments						
BIS	*coeff* = 1.55 *P* = 0.071	*coeff* = 0.031 *P* = 0.026 *	*coeff* = –2.38 *P* = 0.017 *	*coeff* = 1.74 *P* = 0.023*	1.0	0.001
ELF rule violations	*coeff* = 0.25 *P* = 0.12	*coeff* = 0.24 *P* = 0.10	*coeff* = –0.51 *P* = 0.018 *	*coeff* = 0.34 *P* = 0.0050**	1.0	0.001
Delay Discount *k*	*coeff* = 0.033 *P* = 0.67	*coeff* = –0.11 *P* = 0.33	*coeff* = –0.46 *P* = 0.020*	*coeff* = –0.013 *P* = 0.85	1.0	0.001
Post-DBS gambling behaviours						
Bet size	*coeff* = 0.045 *P* = 0.78	*coeff* = 0.35 *P* = 0.056	*coeff* = 0.53 *P* = 0.0050**	*coeff* = 0.37 *P* = 0.059	1.0	0.001

Significance: *$P < 0.05$; **$P < 0.01$; ***$P < 0.001$.
In the cross-lagged model:

(i) $Connectivity_{t1} \rightarrow \Delta Behaviour$ represents connectivity to behaviour coupling: the extent to which structural connectivity at baseline associates with change in impulsivity and gambling at follow-up.

(ii) $Behaviour_{t1} \rightarrow \Delta Connectivity$ represents behaviour to connectivity coupling: the degree of change in structural connectivity dependent on impulsivity at baseline.

(iii) $Connectivity_{t1} \sim Behaviour_{t1}$ is connectivity-behaviour covariance at baseline

(iv) $\Delta Connectivity \sim \Delta Behaviour$ is an estimate of correlated change: reflecting the degree to which connectivity and behaviour changes co-occur.

BIS = Barratt Impulsiveness Scale; CFI = Comparative Fit Index; RMSEA = root mean square error of approximation.

Supplementary Table 7). There was no significant difference by preoperative ICB status ($P = 0.27$) but there was a significant difference in postoperative caseness on the effect of connectivity (coefficient case-positive = –0.90, case-negative = 0.56, $P = 0.020$). The connectivity of the VAT with the reward evaluation network explained 25.7% of the total postoperative variance in bet size. In a linear mixed effects model, an increase in connectivity of 1 standard error (SE) increased bet size by AUD 31.1 [±5.49, $\chi^2(1) = 26.6$, $P = 2.5 \times 10^{-7}$] with no significant covariates.

Baseline connectivity of the reward evaluation circuit did not predict postoperative changes in bet size ($P = 0.78$; Table 3). However, prior to DBS there was a significant relationship between pre-DBS bet size and baseline connectivity (coefficient = 0.53, $P = 0.0050$), with greater connectivity also associated with higher bets. There was no significant correlation in change between gambling and structural connectivity pre- to post-DBS ($P = 0.059$) (Supplementary Fig. 7).

Double or nothing gambles

The likelihood of a gambler taking on a double or nothing gamble was not associated with the structural connectivity of the site of stimulation, when the reward evaluation and response inhibition networks were entered into the PLS path models.

Fibre tracts discriminative of bet size in case-positive and case-negative participants

Subsequently, we used a normative connectome derived from individuals with Parkinson's disease to visualize white matter fibres connected to the stimulation field. We selected fibres predictive of bet size and compared these between case-positive and case-negative participants. This allows identification of fibres associated with gambling behaviour that are also associated with pathological behaviour of a clinically-relevant nature. In case-negative participants, streamlines predictive of increased bet size passed from the diencephalon lateral to the STN and to the right vmPFC and OFC, consistent with findings from the PLS-PM analysis. In the right hemisphere, a portion of these streamlines traversed the VTA. However, in case-positive participants, right-hemispheric fibres predominantly involved the OFC rather than vmPFC. Moreover, these fibres were situated medial to the right STN and appeared to terminate/originate in the STN rather than passing into the midbrain (Fig. 5).

Relationship between motor and neuropsychiatric symptoms

We also investigated whether neuropsychiatric symptoms, including impulsivity, could be dissociated from postoperative improvement in UPDRS part III motor examination scores, given that treatment of motor symptoms is the core clinical objective of STN-DBS for Parkinson's disease. Measures of postoperative impulsivity including the BIS ($r = 0.41$, corrected $P = 0.0048$), the Hayling AB Error Score ($r = 0.42$, corrected $P = 0.0048$) and Double or Nothing Gambles in the virtual casino ($r = 0.42$, corrected $P = 0.0048$) were positively correlated with UPDRS Part III score, suggesting that the greater the impulsivity, the worse were postoperative motor symptoms after STN-DBS (Supplementary Table 8). Moreover, participants who

developed clinically-significant neuropsychiatric symptoms characterized by euphoria, disinhibition and impulsivity (cases) were also more likely to have a lesser postoperative improvement (or worsening) of motor symptoms ($t = 2.53$, mean difference 22 UPDRS points, corrected $P = 0.018$).

To obtain a more sensitive measure of symptomatic change after DBS, we calculated the percentage improvement in motor symptoms post-DBS (stimulation on), as compared to pre-DBS (medication ON). Placing these values into the PLS path models of our frontostriatal networks, improvement in motor symptoms was not related to the structural connectivity of the site of stimulation within the response inhibition network. However, the greater the connectivity of the stimulation field within the reward evaluation network, the lower the improvement in postoperative motor symptoms (coefficient = –0.37, $P = 0.0085$, 95% confidence interval = –0.62 to –0.11).

To evaluate differential effects of focal stimulation within the STN on motor and dimensional neuropsychiatric outcomes, we next analysed the position of the active contact and the distribution of the stimulation field with reference to affective, associative and motor regions of the DISTAL subthalamic atlas. To identify predictive anatomical variables, we first used a variable selection and regularization algorithm, reducing the dimensionality of the dataset and avoiding multiple testing. Candidate variables were then tested in a general linear model controlling for age, gender, LEDD and years since diagnosis of Parkinson's disease. Only percentage change in motor symptoms was found to be related to these subthalamic variables. The closer the active contact to the centroid of the left motor subregion ($z = -8.63$, $P = 0.0025$) and the greater the distribution of the VAT within the left motor subregion ($z = 0.37$, $P = 0.018$), the greater the postoperative reduction in motor symptoms. The variable selection algorithm did not identify predictive variables for the other dimensional assessments of impulsivity (Supplementary Table 9).

Differences in focal subthalamic stimulation and connectivity amongst cases and non-cases

Differences in focal subthalamic stimulation were identified for the categorical delineation of participants into 'cases' and 'non-cases' (Supplementary Table 10). A history of caseness was significantly associated with a closer distance to the centroid of the affective subregion of the right STN ($t = 3.40$, mean difference 2.16 mm, corrected $P = 0.0080$), a further distance from the centroid of the right motor subregion ($t = -4.67$, mean difference 1.92 mm, corrected $P = 0.00030$) and lesser distribution of the stimulation field within the right motor subregion ($t = 3.80$, mean difference 27%, corrected $P = 0.0031$). However, there were no significant differences between cases and non-cases regarding the connectivity of the stimulation field with frontostriatal regions (Supplementary Table 11).

Finally, amongst participants who became cases, we simulated stimulation fields associated with the acute onset of neuropsychiatric symptoms and compared the subthalamic distribution and frontostriatal connectivity of these VATs with those simulated at the 3-month postoperative assessment when acute symptoms had remitted, because of a change in the stimulation parameters and hence the VAT [Fig. 3B(i and ii), Supplementary Tables 1 and 2]. Cases with active symptoms were more likely to have greater stimulation within the right limbic STN subregion ($t = 2.48$, mean difference 10%, uncorrected $P = 0.024$) although this did not survive correction for multiple comparisons (Supplementary Table 12). Furthermore, cases with active symptoms (i.e. before stimulation adjustment) had greater connectivity of the site of stimulation with the right OFC ($t = 3.26$, mean difference 1.49 apparent fibre density units, corrected $P = 0.039$) (Supplementary Table 13). Therefore, changes in the VAT leading to symptom resolution implicated structural connectivity of the stimulation field with the right OFC.

Discussion

In patients with Parkinson's disease undertaking subthalamic DBS, dimensional measures of impulsivity and gambling behaviour covaried with the structural connectivity between the field of stimulation and frontostriatal networks (reward evaluation and response inhibition). The variance explained by connectivity was higher for a behavioural index of impulsivity derived from a virtual casino than for the neuropsychiatric instruments. The relative contribution of white matter tracts in each network differed for each measure, suggesting that impulsivity is a multifactorial construct in this clinical group. Notably, structural connectivity of these networks at baseline (prior to DBS) did not associate with postoperative behaviour, suggesting a primary role for the locus and distribution of stimulation in explaining this variance. Although there were no significant differences in these quantitative assessments of impulsivity amongst individuals who developed clinically-significant postoperative changes in mood and impulsive behaviour (cases), these cases could be discriminated by the interaction of connectivity and betting behaviour in the virtual casino, there being a significant difference in postoperative caseness on the effect of connectivity on bet size. These cases were not able to be discriminated prospectively based on neuropsychiatric or clinical indices, including a background of ICBs prior to STN-DBS.

Postoperatively, inter-individual variability in impulsiveness was best accounted for by a model incorporating the response inhibition network, composed of bilateral fibre tracts connecting the subthalamic VAT with the SMA and IFG. The greater the connectivity of the site of stimulation in this network, the more impulsive and disinhibited were the participants. At baseline, the inverse relationship was observed between connectivity and impulsiveness, but structural connectivity of this 'stopping' network preoperatively (Aron *et al.*, 2007; Rae *et al.*, 2015) did not pre-empt behaviour postoperatively. This finding suggests that if this structural network is incorporated into the stimulation field through placement of the DBS electrode or stimulation titration, the

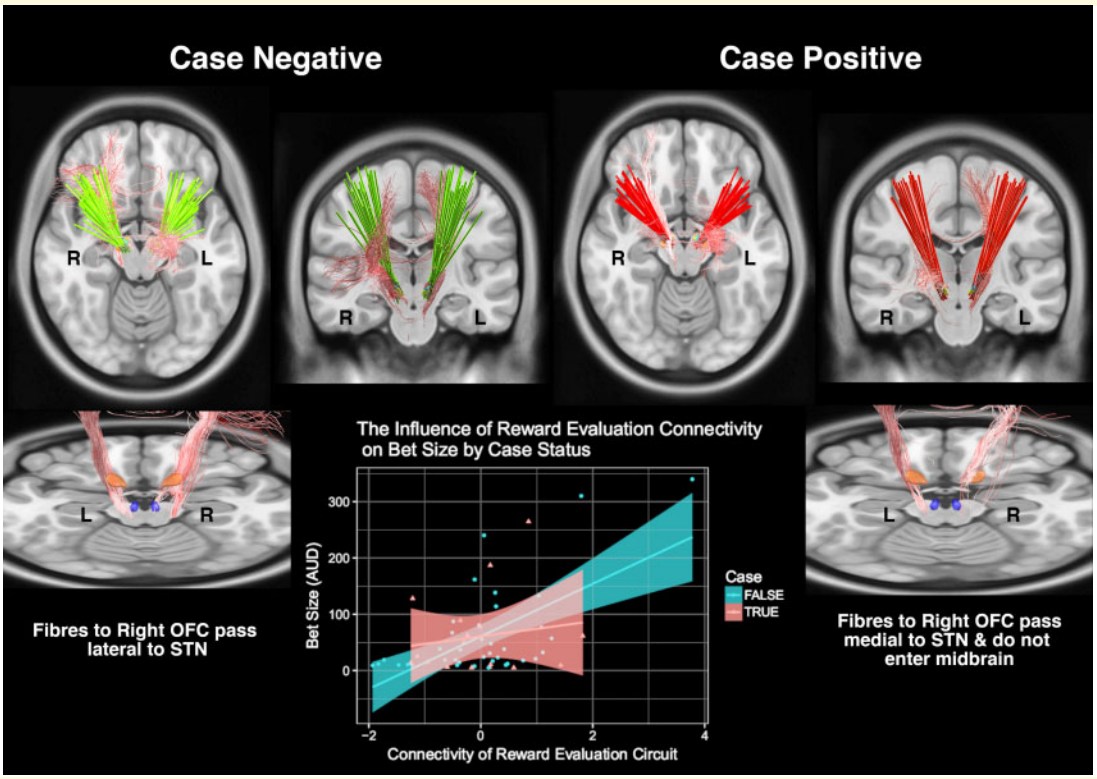

Figure 5 Fibre tracts weighted most strongly in the association of connectivity with gambling. Fibres that were discriminative of bet size and mediated differences between case-positive and case-negative groups. A greater proportion of fibres connecting the right STN with the right OFC were observed in case positive participants. Furthermore, these fibres appeared to run medial rather than lateral to the STN (shown in orange in the *bottom right* and *left* panels) and did not traverse the diencephalon or include the VTA (shown in blue in *bottom right* and *left* panels). The *bottom middle* panel visualizes the relationship between connectivity of the reward evaluation network and bet size, differentiated by caseness.

influence of STN-DBS may be to engender impulsivity. This accords with substantial prior literature connecting STN-DBS to impairment in action restraint (Hershey *et al.*, 2004), action cancellation (Obeso *et al.*, 2013) and task-switching (Witt *et al.*, 2004), and supports prior work providing a structural substrate through which this impairment may arise (Haynes and Haber, 2013). In other words, the change in the effect of connectivity (with opposite effects on behaviour) generated by STN-DBS arises through disruption of the natural functioning of the STN within an inhibitory frontostriatal network. Before DBS, the stronger the connectivity between the STN, IFG and SMA, the lesser the impulsiveness, presumably related to a greater capacity for inhibition conferred by greater connectivity. Postoperatively, the greater the connectivity with the subthalamic VAT (denoting a greater proportion of fibres in this network influenced by the field of high-frequency stimulation) the more compromised are physiological patterns of neural signalling and the more disrupted is the capacity for behavioural inhibition. Based on the latent change score modelling, it appears that the number of fibres recruited by the VAT (which depends on the exact position of the DBS lead and the stimulation parameters) is a more important factor in the evolution of impulsive behaviour than the structure of these networks before surgery.

Inter-individual variability in disinhibition, as manifest with ELF rule violations, was best accounted for by a model incorporating the reward evaluation network—a network composed of bilateral fibre tracts connecting the subthalamic VAT with the ventral striatum, VTA, OFC and vmPFC. The most heavily weighted tract in this network linked the right subthalamic VAT with vmPFC, suggesting that the strength of the stopping signal exerted by the STN makes a key contribution to the behavioural role of this network. This 'hyperdirect' tract may be a means through which the STN links reward evaluation and response inhibition networks (Nambu *et al.*, 2002; Haynes and Haber, 2013). Again, at baseline, the inverse relationship was observed between connectivity and behaviour. The weight of the right-hemisphere in the postoperative network is noteworthy, given prior work suggesting that the executive control of inhibition is primarily a right-lateralized process (Aron *et al.*, 2004; Possin *et al.*, 2009; D'Alberto *et al.*, 2017). These results also support the previous finding that modulation of the right associative STN subregion after DBS for Parkinson's disease is most likely to induce disinhibition (Mosley *et al.*,

2018*c*), with this subregion most likely to show connectivity with the vmPFC in the topographically-organized STN. Again, the change in valence between pre- and postoperative conditions is likely attributable to the disruption (due to high-frequency stimulation) of the physiological 'stopping' signal provided by the STN, in particular to the vmPFC.

Inter-individual variability in impatience was also best explained by the connectivity of the reward evaluation network. Here, there was no dissociation by valence pre- and post-DBS; at both intervals stronger network connectivity was associated with a greater ability to delay gratification in the service of a larger reward. However, the variance explained by connectivity was small for this measure.

For two neuropsychiatric outcomes, the QUIP-RS and the Hayling AB Error Score, there was no significant relationship between inter-individual variability and structural network connectivity with the participant-specific stimulation field. For the QUIP-RS, it may be that the substantial postoperative reduction in dopaminergic medication affects measurement of this construct, given that STN-DBS (with its attendant reduction in LEDD) has been advanced as a treatment for compulsivity (Lhommee *et al.*, 2012; Eusebio *et al.*, 2013). In the Hayling test, it may be that the AB error score is too coarse a measurement of disinhibition, given that a finer-grained analysis of this instrument has shown differing anatomical specificity of A and B errors (Robinson *et al.*, 2015; Cipolotti *et al.*, 2016). Further work will be necessary to understand these findings.

Brain-behaviour covariations were stronger for betting behaviour in the virtual casino than for the neuropsychiatric instruments. The greater the connectivity of the subthalamic VAT with the reward evaluation network, the higher the bets made by participants, with an increase of 1 SE in connectivity associated with an increased bet of AUD 31.1. The involvement of bilateral tracts connecting the site of stimulation with OFC is particularly interesting given the role of this region in predicting outcomes after behavioural choices (Rudebeck and Murray, 2014) and contributing to prediction error signalling in ascending dopaminergic projections from the VTA (Takahashi *et al.*, 2011). This also lends further support to the idea that spread of electrical stimulation into ventromedial regions of the STN can quantitatively influence impulsivity.

An alternative explanation for these findings is that the subthalamic VAT modulates ascending dopaminergic fibres in the superolateral branch of the medial forebrain bundle (slMFB), which pass adjacent to the STN and onwards to vmPFC and OFC (Coenen *et al.*, 2009, 2012). Lateral orbitofrontal branches of the slMFB traverse the ventral striatum via the anterior limb of the internal capsule, potentially explaining why the ventral striatum is also weighted heavily in the reward evaluation network for bet size (Coenen *et al.*, 2018). Appetitive learning and reinforcement are underpinned by dopaminergic signalling within mesocorticolimbic networks (Haber and Knutson, 2010) and it is plausible that STN-DBS could directly affect the evaluation of reward in this manner outside of any direct effect on STN firing.

The distinction observed between case-positive and case-negative participants in the effect of connectivity on bet size offers an insight into these alternative hypotheses. In case-negative individuals, the effect of connectivity has a strong positive valence, whilst visual inspection of individual discriminative fibres isolated from a normative connectome shows ascending tracts passing through the VTA and adjacent to the STN in the right hemisphere, distributed widely amongst vmPFC and OFC. Therefore, in such individuals, it is plausible that direct modulation of the slMFB is operating to mediate this relationship. However, in case-positive individuals, this relationship between connectivity and bet size is not observed. Visual inspection of discriminative fibres shows tracts between the STN and right OFC that do not extend into the diencephalon. These fibres conceivably represent direct cortical-STN connections that drive STN output and behavioural inhibition. These findings converge with our previous work demonstrating that ventromedial dispersion of the stimulation field within the right STN was more likely to be associated with disinhibition and the development of clinically-significant hypomania and harmful impulsivity (Mosley *et al.*, 2018*c*). Furthermore, our finding that cases with active neuropsychiatric symptoms differed in the connectivity of the stimulation field with the right OFC further implicates this prefrontal region in the genesis of these clinically-significant behavioural changes.

More generally, our finding that participants with clinically-significant neuropsychiatric symptoms after STN-DBS did not differ from other participants on raw behavioural indices derived from the virtual casino, aligns with recent work demonstrating a more nuanced relationship between connectivity and behaviour in Parkinson's disease. In a previous study of non-surgical patients with Parkinson's disease (Mosley *et al.*, 2019*a*), we found no difference in gambling behaviours between participants with and without a history of ICBs. However, we observed a scaling of structural connectivity in the reward evaluation network and impulsive gambling in the virtual casino, which was present only amongst participants without ICBs and not amongst those with ICBs. The observed differences in the scaling of connectivity and behaviour between clinical groups such as these may progress the neuroimaging-based identification of patients vulnerable to neuropsychiatric complications of treatment.

An important question is whether optimal improvement in motor symptoms after STN-DBS is correlated or anti-correlated with impulsive behaviour. In other words, is impulsivity an unfortunate but unavoidable corollary of the relief of akinesia, rigidity and tremor? Or alternatively, does impulsivity suggest a suboptimal focal stimulation profile or suboptimal pattern of network modulation (Volkmann *et al.*, 2010)? Our results suggest that motor and non-motor symptoms were dissociable in this cohort. Impulsive participants were more likely to have worse motor symptoms after DBS and frontostriatal network modulation was also associated with a lesser improvement (or worsening) of motor symptoms postoperatively. Additionally, improvement in motor

symptoms was associated with greater stimulation of the motor subregion of the STN, whilst dimensional neuropsychiatric variables showed no association with focal STN stimulation. Furthermore, the development of clinically-significant neuropsychiatric symptoms (caseness) was associated with greater motor symptoms, as well as with greater stimulation of the right associative STN and lesser stimulation of the right motor subregion. Overall, these findings imply the existence of a connectivity target that could optimize motor symptoms whilst minimizing neuropsychiatric side effects. These findings are also supported by prior work in which stimulation of the hyperdirect pathway between the STN and pre-SMA was not associated with improved motor symptoms, but did lead to faster reaction times with more erroneous movements (i.e. impulsive and error-prone) in a complex motor task requiring inhibitory control (Neumann *et al.*, 2018). Modulation of the effectivity connectivity in the hyperdirect pathway between STN and cortex has also been associated with a reduction in the clinical effectiveness of STN-DBS (Kahan *et al.*, 2014). Optimal patterns ('sweet spots') of focal stimulation, in addition to structural and functional signatures of effective subthalamic stimulation have been defined with reference to the anti-parkinsonian effects of STN-DBS (Akram *et al.*, 2017; Horn *et al.*, 2017, 2019*b*; Dembek *et al.*, 2019). It is anticipated that these will continue to be refined to incorporate neuropsychiatric indices.

A related question is whether it is stimulation of the target nucleus that leads to neuropsychiatric side effects, or whether dispersion of the stimulation field outside of the STN modulates adjacent fibre tracts responsible for these symptoms. The clinical relevance of this question again pertains to targeting and stimulation titration: can neuropsychiatric symptoms be avoided by more accurate electrode placement and focal stimulation only within the STN? The association between focal stimulation of the motor STN subregion and improvement in motor symptoms, as well as the relationship of ascending tegmental fibres with bet size in the virtual casino also suggests a dissociation here. Whilst the highest probability of stimulation in our cohort was within the dorsolateral region of the STN (Fig. 3), inevitably there is dispersion of charge into the surrounding tissue. However, we cannot definitively resolve this question with our connectivity analysis, which is agnostic to the origin of fibre projections and the mechanism of DBS at the cellular level.

A number of caveats need to be considered when interpreting these results. First, although we found that the structural connectivity of frontostriatal networks at baseline did not associate with postoperative changes in impulsivity, it is important to note that we did not model all potentially-relevant demographic and disease-related covariates in the latent change score models. We opted for a more parsimonious representation, with the aim of characterizing a structural signal of vulnerability to postoperative impairment and avoiding statistical complexity. Moreover, we note that these covariates were not found to have a significant relationship with postoperative behaviour in the PLS-PM analyses or linear mixed effects modelling (only years since diagnosis of Parkinson's disease affected Delay Discount performance). Second, our case-positive participants were assessed after stimulation manipulation had taken place to remediate more florid neuropsychiatric symptoms. Therefore, the distribution of stimulation associated with clinical hypomania will have been slightly different to that recorded at the formal postoperative assessment. However, we could still discriminate these groups in our virtual casino even after resolution of clinically-significant symptoms, based on the relationship between connectivity and bet size. This suggests that our assay was relatively sensitive and arguably improves the robustness of our findings. Third, the methodology employed in the isolation of discriminative fibres from the normative connectome involved mass-univariate tests across many connected fibres without controlling for the false discovery rate and thus must be viewed with caution. Finally, our method of assessing improvement in motor symptoms by comparing medication ON (prior to DBS) and stimulation on (after DBS) was not optimal in this regard (ideally motor symptoms should be assessed 'off' and 'on' at both intervals). However, we found that our participants were too impaired to tolerate a drug/stimulation washout as well as complete the extensive battery of neuropsychiatric instruments. Similarly, assessing performance on these instruments and the virtual casino both on and off DBS was prohibited by the emergence of severe motor symptoms in this cohort once stimulation was interrupted. This necessarily limits definitive conclusions regarding the role of electrical stimulation in disrupting these non-motor networks. Future work targeting a younger, less severely-affected cohort might permit such an on/off design.

In conclusion, STN-DBS is an established and valuable intervention for the motor symptoms of Parkinson's disease. However, there are relatively frequent and important neuropsychiatric changes which affect postoperative quality of life. We have demonstrated that the structural connectivity of the site of stimulation with reward evaluation and response inhibition networks is a major determinant of dimensional variability in postoperative impulsivity. Our results also suggest that the connectivity of the stimulation field with the prefrontal cortex (specifically the OFC) relates to the development of categorical changes in mood and behaviour of clinical significance. Structural connectivity of these networks at baseline was not associated with postoperative neuropsychiatric outcomes, suggesting that electrode placement and accurate stimulation titration are key drivers of these non-motor outcomes, over-riding and even reversing preoperative effects. It further highlights the difficulty of identifying an 'at-risk' phenotype prior to neurosurgery. In summary, the lack of a preoperative connectivity 'fingerprint' signifying susceptibility to postoperative impulsive behaviour is of clinical relevance to surgical teams planning STN-DBS for Parkinson's disease, because it suggests that neuropsychiatric side-effects, as well as symptomatic benefit, arise from the modulatory effects of the stimulation field on

connected networks. As more neurosurgical centres employ tractography to improve DBS electrode targeting, contact selection and current steering for Parkinson's disease, we anticipate that these findings will assist with adapting these methods to address neuropsychiatric outcomes.

Acknowledgements

The authors gratefully acknowledge the commitment of participants and caregivers who contributed their time to this study. The authors acknowledge the ongoing support of St Andrew's War Memorial Hospital and the Herston Imaging Research Facility. The authors thank Till Dembek for assistance with modelling the field of stimulation in directional leads.

Funding

P.E.M. was supported by an early career fellowship from the Queensland government's 'Advance Queensland' initiative, a Royal Brisbane and Woman's Hospital Foundation Research Grant and a young investigator grant from the Royal Australian and New Zealand College of Psychiatrists. He received an unrestricted educational grant from Medtronic. M.B. was supported by the National Health and Medical Research Council (118153, 10371296, 1095227) and the Australian Research Council (CE140100007). K.E.S. was supported by the University of Zurich and the René and Susanne Braginsky Foundation. A.P. acknowledges the current support of Dr Douglas Garrett's funding from the Emmy Noether Programme grant (German Research Council) and the Max Planck UCL Centre for Computational Psychiatry and Ageing Research.

Competing interests

The authors report no competing interests.

Supplementary material

Supplementary material is available at *Brain* online.

References

Accolla EA, Dukart J, Helms G, Weiskopf N, Kherif F, Lutti A, et al. Brain tissue properties differentiate between motor and limbic basal ganglia circuits. Hum Brain Mapp 2014; 35: 5083–92.

Accolla EA, Herrojo Ruiz M, Horn A, Schneider GH, Schmitz-Hubsch T, Draganski B, et al. Brain networks modulated by subthalamic nucleus deep brain stimulation. Brain 2016; 139: 2503–15.

Akram H, Sotiropoulos SN, Jbabdi S, Georgiev D, Mahlknecht P, Hyam J, et al. Subthalamic deep brain stimulation sweet spots and hyperdirect cortical connectivity in Parkinson's disease. Neuroimage 2017; 158: 332–45.

Antonelli F, Ko JH, Miyasaki J, Lang AE, Houle S, Valzania F, et al. Dopamine-agonists and impulsivity in Parkinson's disease: impulsive choices vs. impulsive actions. Hum Brain Mapp 2014; 35: 2499–506.

Appleby BS, Duggan PS, Regenberg A, Rabins PV. Psychiatric and neuropsychiatric adverse events associated with deep brain stimulation: a meta-analysis of ten years' experience. Mov Disord 2007; 22: 1722–8.

Aron AR, Behrens TE, Smith S, Frank MJ, Poldrack RA. Triangulating a cognitive control network using diffusion-weighted magnetic resonance imaging (MRI) and functional MRI. J Neurosci 2007; 27: 3743–52.

Aron AR, Robbins TW, Poldrack RA. Inhibition and the right inferior frontal cortex. Trends Cogn Sci 2004; 8: 170–7.

Avants BB, Epstein CL, Grossman M, Gee JC. Symmetric diffeomorphic image registration with cross-correlation: evaluating automated labeling of elderly and neurodegenerative brain. Med Image Anal 2008; 12: 26–41.

Baldermann JC, Melzer C, Zapf A, Kohl S, Timmermann L, Tittgemeyer M, et al. Connectivity profile predictive of effective deep brain stimulation in obsessive-compulsive disorder. Biol Psychiatry 2019; 85: 735–43.

Bates D, Machler M, Bolker BM, Walker SC. Fitting linear mixed-effects models using lme4. J Stat Soft 2015; 67: 1–48.

Beck AT, Ward CH, Mendelson M, Mock J, Erbaugh J. An inventory for measuring depression. Arch Gen Psychiatry 1961; 4: 561–71.

Benjamini Y, Hochberg Y. Controlling the false discovery rate: a practical and powerful approach to multiple testing. J R Stat Soc Seri B Methodol 1995; 57: 289–300.

Burgess PW, Shallice T. Thames valley test company. The Hayling and Brixton tests. Bury St Edmunds: Thames Valley Test Company; 1997. [Database]

Cavanagh JF, Wiecki TV, Cohen MX, Figueroa CM, Samanta J, Sherman SJ, et al. Subthalamic nucleus stimulation reverses mediofrontal influence over decision threshold. Nat Neurosci 2011; 14: 1462–7.

Chen Y, Ge S, Li Y, Li N, Wang J, Wang X, et al. Role of the cortico-subthalamic hyperdirect pathway in deep brain stimulation for the treatment of Parkinson disease: a diffusion tensor imaging study. World Neurosurg 2018; 114: e1079–e85.

Cipolotti L, Healy C, Spano B, Lecce F, Biondo F, Robinson G, et al. Strategy and suppression impairments after right lateral prefrontal and orbito-frontal lesions. Brain 2016; 139: e10.

Coenen VA, Honey CR, Hurwitz T, Rahman AA, McMaster J, Burgel U, et al. Medial forebrain bundle stimulation as a pathophysiological mechanism for hypomania in subthalamic nucleus deep brain stimulation for Parkinson's disease. Neurosurgery 2009; 64: 1106–14. discussion 14–5.

Coenen VA, Panksepp J, Hurwitz TA, Urbach H, Madler B. Human medial forebrain bundle (MFB) and anterior thalamic radiation (ATR): imaging of two major subcortical pathways and the dynamic balance of opposite affects in understanding depression. J Neuropsychiatry Clinc Neurosci 2012; 24: 223–36.

Coenen VA, Schumacher LV, Kaller C, Schlaepfer TE, Reinacher PC, Egger K, et al. The anatomy of the human medial forebrain bundle: ventral tegmental area connections to reward-associated subcortical and frontal lobe regions. Neuroimage Clin 2018; 18: 770–83.

Daniele A, Albanese A, Contarino MF, Zinzi P, Barbier A, Gasparini F, et al. Cognitive and behavioural effects of chronic stimulation of the subthalamic nucleus in patients with Parkinson's disease. J Neurol Neurosurg Psychiatry 2003; 74: 175–82.

Dembek TA, Roediger J, Horn A, Reker P, Oehrn C, Dafsari HS, et al. Probabilistic sweet spots predict motor outcome for deep brain stimulation in Parkinson disease. Ann Neurol 2019; 86: 527–38.

Doll BB, Frank MJ. Chapter 19 - The basal ganglia in reward and decision making: computational models and empirical studies. In: J-C Dreher, L Tremblay, editors. Handbook of reward and decision making. New York: Academic Press; 2009. p. 399–425.

D'Alberto N, Funnell M, Potter A, Garavan H. A split-brain case study on the hemispheric lateralization of inhibitory control. Neuropsychologia 2017; 99: 24–9.
Edlow BL, Mareyam A, Horn A, Polimeni JR, Witzel T, Tisdall MD, et al. 7 Tesla MRI of the ex vivo human brain at 100 micron resolution. Sci Data 2019; 6: 244.
Emre M, Aarsland D, Brown R, Burn DJ, Duyckaerts C, Mizuno Y, et alet al. Clinical diagnostic criteria for dementia associated with Parkinson's disease. Mov Disord 2007; 22: 1689–707.
Eusebio A, Pogosyan A, Wang S, Averbeck B, Gaynor LD, Cantiniaux S, et al. Resonance in subthalamo-cortical circuits in Parkinson's disease. Brain 2009; 132: 2139–50.
Eusebio A, Thevathasan W, Doyle Gaynor L, Pogosyan A, Bye E, Foltynie T, et al. Deep brain stimulation can suppress pathological synchronisation in Parkinsonian patients. J Neurol Neurosurg Psychiatry 2011; 82: 569–73.
Eusebio A, Witjas T, Cohen J, Fluchere F, Jouve E, Regis J, et al. Subthalamic nucleus stimulation and compulsive use of dopaminergic medication in Parkinson's disease. J Neurol Neurosurg Psychiatry 2013; 84: 868–74.
Evans AH, Katzenschlager R, Paviour D, O'Sullivan JD, Appel S, Lawrence AD, et al. Punding in Parkinson's disease: its relation to the dopamine dysregulation syndrome. Mov Disord 2004; 19: 397–405.
Ewert S, Plettig P, Li N, Chakravarty MM, Collins DL, Herrington TM, et al. Toward defining deep brain stimulation targets in MNI space: a subcortical atlas based on multimodal MRI, histology and structural connectivity. Neuroimage 2018; 170: 271–82.
Folstein MF, Folstein SE, McHugh PR. "Mini-mental state". A practical method for grading the cognitive state of patients for the clinician. J Psychiatric Res 1975; 12: 189–98.
Frank MJ, Samanta J, Moustafa AA, Sherman SJ. Hold your horses: impulsivity, deep brain stimulation, and medication in Parkinsonism. Science 2007; 318: 1309–12.
Friedman J, Hastie T, Tibshirani R. Regularization paths for generalized linear models via coordinate descent. J Stat Soft 2010; 33: 1–22.
Haber SN, Knutson B. The reward circuit: linking primate anatomy and human imaging. Neuropsychopharmacol 2010; 35: 4–26.
Hampton WH, Alm KH, Venkatraman V, Nugiel T, Olson IR. Dissociable frontostriatal white matter connectivity underlies reward and motor impulsivity. Neuroimage 2017; 150: 336–43.
Hastie T, Tibshirani R, Friedman JH. The elements of statistical learning: data mining, inference, and prediction. 2nd edn. New York, NY: Springer; 2009.
Haynes WI, Haber SN. The organization of prefrontal-subthalamic inputs in primates provides an anatomical substrate for both functional specificity and integration: implications for Basal Ganglia models and deep brain stimulation. J Neurosci 2013; 33: 4804–14.
Hellerbach A, Dembek TA, Hoevels M, Holz JA, Gierich A, Luyken K, et al. DiODe: directional orientation detection of segmented deep brain stimulation leads: a sequential algorithm based on CT imaging. Stereotact Funct Neurosurg 2018; 96: 335–41.
Hershey T, Campbell MC, Videen TO, Lugar HM, Weaver PM, Hartlein J, et al. Mapping Go-No-Go performance within the subthalamic nucleus region. Brain 2010; 133: 3625–34.
Hershey T, Revilla FJ, Wernle A, Gibson PS, Dowling JL, Perlmutter JS. Stimulation of STN impairs aspects of cognitive control in PD. Neurology 2004; 62: 1110–4.
Hoehn MM, Yahr MD.Parkinsonism: onset, progression, and mortality. Neurology 1967; 17: 427–42.
Horn A, Kuhn AA. Lead-DBS: a toolbox for deep brain stimulation electrode localizations and visualizations. Neuroimage 2015; 107: 127–35.
Horn A, Li N, Dembek TA, Kappel A, Boulay C, Ewert S, et al. Lead-DBS v2: towards a comprehensive pipeline for deep brain stimulation imaging. Neuroimage 2019a; 184: 293–316.
Horn A, Reich M, Vorwerk J, Li N, Wenzel G, Fang Q, et al. Connectivity Predicts deep brain stimulation outcome in Parkinson disease. Ann Neurol 2017; 82: 67–78.
Horn A, Wenzel G, Irmen F, Huebl J, Li N, Neumann WJ, et al. Deep brain stimulation induced normalization of the human functional connectome in Parkinson's disease. Brain 2019b; 142: 3129–43.
Hughes AJ, Daniel SE, Kilford L, Lees AJ.Accuracy of clinical diagnosis of idiopathic Parkinson's disease: a clinico-pathological study of 100 cases. J Neurol Neurosurg Psychiatry 1992; 55: 181–4.
Hughes LE, Rittman T, Robbins TW, Rowe JB. Reorganization of cortical oscillatory dynamics underlying disinhibition in frontotemporal dementia. Brain 2018; 141: 2486–99.
Jeurissen B, Tournier JD, Dhollander T, Connelly A, Sijbers J. Multi-tissue constrained spherical deconvolution for improved analysis of multi-shell diffusion MRI data. Neuroimage 2014; 103: 411–26.
Kahan J, Urner M, Moran R, Flandin G, Marreiros A, Mancini L, et al. Resting state functional MRI in Parkinson's disease: the impact of deep brain stimulation on 'effective' connectivity. Brain 2014; 137: 1130–44.
Kievit RA, Brandmaier AM, Ziegler G, van Harmelen AL, de Mooij SMM, Moutoussis M, et al. Developmental cognitive neuroscience using latent change score models: a tutorial and applications. Dev Cogn Neurosci 2018; 33: 99–117.
Kirby KN, Petry NM, Bickel WK. Heroin addicts have higher discount rates for delayed rewards than non-drug-using controls. J Exp Psychol Gen 1999; 128: 78–87.
Krack P, Batir A, Van Blercom N, Chabardes S, Fraix V, Ardouin C, et al. Five-year follow-up of bilateral stimulation of the subthalamic nucleus in advanced Parkinson's disease. N Engl J Med 2003; 349: 1925–34.,
Lambert C, Zrinzo L, Nagy Z, Lutti A, Hariz M, Foltynie T, et al. Confirmation of functional zones within the human subthalamic nucleus: patterns of connectivity and sub-parcellation using diffusion weighted imaging. Neuroimage 2012; 60: 83–94.
Lhommee E, Klinger H, Thobois S, Schmitt E, Ardouin C, Bichon A, et al. Subthalamic stimulation in Parkinson's disease: restoring the balance of motivated behaviours. Brain 2012; 135: 1463–77.
Lim SY, O'Sullivan SS, Kotschet K, Gallagher DA, Lacey C, Lawrence AD, et al. Dopamine dysregulation syndrome, impulse control disorders and punding after deep brain stimulation surgery for Parkinson's disease. J Clin Neurosci 2009; 16: 1148–52.
Lin HY, Perry A, Cocchi L, Roberts JA, Tseng WI, Breakspear M, et al. Development of frontoparietal connectivity predicts longitudinal symptom changes in young people with autism spectrum disorder. Transl Psychiatry 2019; 9: 86.
Mallet L, Schupbach M, N'Diaye K, RP, Bardinet E, Czernecki V, et al. Stimulation of subterritories of the subthalamic nucleus reveals its role in the integration of the emotional and motor aspects of behavior. Proc Natl Acad Sci USA 2007; 104: 10661–6.
McIntosh AR, Lobaugh NJ. Partial least squares analysis of neuroimaging data: applications and advances. Neuroimage 2004; 23 (Suppl 1): S250–63.
Mevik B-H. The pls Package: principal Component and Partial Least Squares Regression in R. J Stat Soft 2007; 18: 1–23.
Mosley PE, Breakspear M, Coyne T, Silburn P, Smith D. Caregiver burden and caregiver appraisal of psychiatric symptoms are not modulated by subthalamic deep brain stimulation for Parkinson's disease. NPJ Parkinsons Dis 2018a; 4: 12.
Mosley PE, Marsh R. The psychiatric and neuropsychiatric symptoms after subthalamic stimulation for Parkinson's Disease. J Neuropsychiatry Cinc Neurosci 2015; 27: 19–26.
Mosley PE, Marsh R, Perry A, Coyne T, Silburn P. Persistence of mania after cessation of stimulation following subthalamic deep brain stimulation. J Neuropsychiatry Clinc Neurosci 2018b; 30: 246–9.
Mosley PE, Paliwal S, Robinson K, Coyne T, Silburn P, Tittgemeyer M, et al. The structural connectivity of discrete networks underlies

impulsivity and gambling in Parkinson's disease. Brain 2019a; 142: 3917–35.
Mosley PE, Robinson K, Coyne T, Silburn P, Breakspear M, Carter A. 'Woe betides anybody who tries to turn me down.' A qualitative analysis of neuropsychiatric symptoms following subthalamic deep brain stimulation for Parkinson's disease. Neuroethics 2019b.
Mosley PE, Smith D, Coyne T, Silburn P, Breakspear M, Perry A. The site of stimulation moderates neuropsychiatric symptoms after subthalamic deep brain stimulation for Parkinson's disease. Neuroimage: Clin 2018c; 18: 996–1006.
Moum SJ, Price CC, Limotai N, Oyama G, Ward H, Jacobson C, et al. Effects of STN and GPi deep brain stimulation on impulse control disorders and dopamine dysregulation syndrome. PloS One 2012; 7: e29768.
Muetzel RL, Blanken LME, van der Ende J, El Marroun H, Shaw P, Sudre G, et al. Tracking brain development and dimensional psychiatric symptoms in children: A longitudinal population-based neuroimaging study. Am J Psychiatry 2018; 175: 54–62.
Nambu A, Tokuno H, Takada M. Functional significance of the cortico-subthalamo-pallidal 'hyperdirect' pathway. Neurosci Res 2002; 43: 111–7.
Nasreddine ZS, Phillips NA, Bedirian V, Charbonneau S, Whitehead V, Collin I, et al. The montreal cognitive assessment, MoCA: a brief screening tool for mild cognitive impairment. J Am Geriatr Soc 2005; 53: 695–9.
Neumann WJ, Schroll H, de Almeida Marcelino AL, Horn A, Ewert S, Irmen F, et al. Functional segregation of basal ganglia pathways in Parkinson's disease. Brain 2018; 141: 2655–69.
Obeso I, Wilkinson L, Rodriguez-Oroz MC, Obeso JA, Jahanshahi M. Bilateral stimulation of the subthalamic nucleus has differential effects on reactive and proactive inhibition and conflict-induced slowing in Parkinson's disease. Exp Brain Res 2013; 226: 451–62.
Odekerken VJ, van Laar T, Staal MJ, Mosch A, Hoffmann CF, Nijssen PC, et al. Subthalamic nucleus versus globus pallidus bilateral deep brain stimulation for advanced Parkinson's disease (NSTAPS study): a randomised controlled trial. Lancet Neurol 2013; 12: 37–44.
Okun MS, Foote KD. Subthalamic nucleus vs globus pallidus interna deep brain stimulation, the rematch: will pallidal deep brain stimulation make a triumphant return? Arch Neurol 2005; 62: 533–6.
Paliwal S, Mosley PE, Breakspear M, Coyne T, Silburn P, Aponte E, et al. Subjective estimates of uncertainty during gambling and impulsivity after subthalamic deep brain stimulation for Parkinson's disease. Sci Rep 2019; 9: 14795.
Paliwal S, Petzschner FH, Schmitz AK, Tittgemeyer M, Stephan KE. A model-based analysis of impulsivity using a slot-machine gambling paradigm. Front Hum Neurosci 2014; 8: 428.
Patton JH, Stanford MS. Barratt Es Factor structure of the Barratt impulsiveness scale. J Clin Psychol 1995; 51: 768–74.
Petry-Schmelzer JN, Krause M, Dembek Ta Horn A, Evans J, Ashkan K, et al. Non-motor outcomes depend on location of neurostimulation in Parkinson's disease. Brain 2019.
Possin KL, Brambati SM, Rosen HJ, Johnson JK, Pa J, Weiner MW, et al. Rule violation errors are associated with right lateral prefrontal cortex atrophy in neurodegenerative disease. J Int Neuropsychol Soc 2009; 15: 354–64.
R Core Team. R: a language and environment for statistical computing. Vienna, Austria: R Foundation for Statistical Computing; 2014.
Rae CL, Hughes LE, Anderson MC, Rowe JB. The prefrontal cortex achieves inhibitory control by facilitating subcortical motor pathway connectivity. J Neurosci 2015; 35: 786–94.
Raffelt D, Tournier JD, Rose S, Ridgway GR, Henderson R, Crozier S, et al. Apparent Fibre Density: a novel measure for the analysis of diffusion-weighted magnetic resonance images. Neuroimage 2012; 59: 3976–94.
Robinson GA, Cipolotti L, Walker DG, Biggs V, Bozzali M, Shallice T. Verbal suppression and strategy use: a role for the right lateral prefrontal cortex?. Brain 2015; 138: 1084–96.
Romito LM, Raja M, Daniele A, Contarino MF, Bentivoglio AR, Barbier A, et al. Transient mania with hypersexuality after surgery for high frequency stimulation of the subthalamic nucleus in Parkinson's disease. Mov Disord 2002; 17: 1371–4.
Rosseel Y. lavaan: An R Package for Structural Equation Modeling. J Stat Softw 2012; 1: 2012.
Rudebeck PH, Murray EA. The orbitofrontal oracle: cortical mechanisms for the prediction and evaluation of specific behavioral outcomes. Neuron 2014; 84: 1143–56.
Sanchez G. PLS path modeling with R. Berkeley, CA: Trowchez Editions; 2013.
Schuepbach WM, Rau J, Knudsen K, Volkmann J, Krack P, Timmermann L, et al. Neurostimulation for Parkinson's disease with early motor complications. N Engl J Med 2013; 368: 610–22.
Shaw P, Weingart D, Bonner T, Watson B, Park MT, Sharp W, et al. Defining the neuroanatomic basis of motor coordination in children and its relationship with symptoms of attention-deficit/hyperactivity disorder. Psychol Med 2016; 46: 2363–73.
Shimamoto SA, Ryapolova-Webb ES, Ostrem JL, Galifianakis NB, Miller KJ, Starr PA. Subthalamic nucleus neurons are synchronized to primary motor cortex local field potentials in Parkinson's disease. J Neurosci 2013; 33: 7220–33.
Shores EA, Carstairs JR, Crawford JR. Excluded Letter Fluency Test (ELF): norms and test–retest reliability data for healthy young adults. Brain Impairment 2006; 7: 26–32.
Spiegel J, Hellwig D, Samnick S, Jost W, Mollers MO, Fassbender K, et al. Striatal FP-CIT uptake differs in the subtypes of early Parkinson's disease. J Neural Transm 2007; 114: 331–5.
Starkstein SE, Mayberg HS, Preziosi TJ, Andrezejewski P, Leiguarda R, Robinson RG. Reliability, validity, and clinical correlates of apathy in Parkinson's disease. J Neuropsychiatry Clin Neurosci 1992; 4: 134.
Takahashi YK, Roesch MR, Wilson RC, Toreson K, O'Donnell P, Niv Y, et al. Expectancy-related changes in firing of dopamine neurons depend on orbitofrontal cortex. Nat Neurosci 2011; 14: 1590–7.
Tournier JD, Calamante F, Connelly A. Robust determination of the fibre orientation distribution in diffusion MRI: non-negativity constrained super-resolved spherical deconvolution. Neuroimage 2007; 35: 1459–72.
Tournier JD, Calamante F, Connelly A, Improved probabilistic streamlines tractography by 2nd order integration over fibre orientation distributions. In: Proceedings of the International Society for Magnetic Resonance in Medicine. Stockholm; 2010.
Tournier JD, Calamante F, Gadian DG, Connelly A. Direct estimation of the fiber orientation density function from diffusion-weighted MRI data using spherical deconvolution. Neuroimage 2004; 23: 1176–85.
van Eimeren T, Pellecchia G, Cilia R, Ballanger B, Steeves TD, Houle S, et al. Drug-induced deactivation of inhibitory networks predicts pathological gambling in PD. Neurology 2010; 75: 1711–6.
Vanegas-Arroyave N, Lauro PM, Huang L, Hallett M, Horovitz SG, Zaghloul KA, et al. Tractography patterns of subthalamic nucleus deep brain stimulation. Brain 2016; 139: 1200–10.
Volkmann J, Daniels C, Witt K. Neuropsychiatric effects of subthalamic neurostimulation in Parkinson disease. Nat Rev Neurol 2010; 6: 487–98.
Voon V, Kubu C, Krack P, Houeto JL, Troster AI. Deep brain stimulation: neuropsychological and neuropsychiatric issues. Mov Disord 2006; 21 (Suppl 14): S305–27.
Vorwerk J, Oostenveld R, Piastra MC, Magyari L, Wolters CH. The FieldTrip-SimBio pipeline for EEG forward solutions. Biomed Eng Online 2018; 17: 37.
Weintraub D, Mamikonyan E, Papay K, Shea JA, Xie SX, Siderowf A. Questionnaire for impulsive-compulsive disorders in Parkinson's Disease–Rating Scale. Mov Disord 2012; 27: 242–7.
Welter ML, Schupbach M, Czernecki V, Karachi C, Fernandez-Vidal S, Golmard JL, et al. Optimal target localization for subthalamic stimulation in patients with Parkinson disease. Neurology 2014; 82: 1352–61.

Williams A, Gill S, Varma T, Jenkinson C, Quinn N, Mitchell R, et al. Deep brain stimulation plus best medical therapy versus best medical therapy alone for advanced Parkinson's disease (PD SURG trial): a randomised, open-label trial. Lancet Neurol 2010; 9: 581–91.

Witt K, Pulkowski U, Herzog J, Lorenz D, Hamel W, Deuschl G, et al. Deep brain stimulation of the subthalamic nucleus improves cognitive flexibility but impairs response inhibition in Parkinson disease. Arch Neurol 2004; 61: 697–700.

Xia M, Wang J, He Y. BrainNet Viewer: a network visualization tool for human brain connectomics. PloS One 2013; 8: e68910.

Yeh F, Wedeen VJ, Tseng WI. Generalized Q-sampling imaging. IEEE Trans Med Imaging 2010; 29: 1626–35.